ANY-ORDER FLEXIBLE LENGTH MASKED DIFFUSION

Jaeyeon Kim^{1,★} Lee Cheuk-Kit^{1, 2,★} Carles Domingo-Enrich³ Yilun Du^{1,2}

Sham Kakade^{1,2} Timothy Ngotiaoco^{1,2} Sitan Chen^{1,†} Michael S. Albergo^{1,2,4,†}

ABSTRACT

Masked diffusion models (MDMs) have recently emerged as a promising alternative to autoregressive models over discrete domains. MDMs generate sequences in an any-order, parallel fashion, enabling fast inference and strong performance on non-causal tasks. However, a crucial limitation is that they do not support token insertions and are thus limited to *fixed-length* generations. To this end, we introduce Flexible Masked Diffusion Models (FlexMDMs), a discrete diffusion paradigm that simultaneously can model sequences of flexible length while provably retaining MDMs' flexibility of any-order inference. Grounded in an extension of the stochastic interpolant framework, FlexMDMs generate sequences by inserting mask tokens and unmasking them. Empirically, we show that FlexMDMs match MDMs in perplexity while modeling length statistics with much higher fidelity. On a synthetic maze planning task, they achieve $\approx 60\%$ higher success rate than MDM baselines. Finally, we show pretrained MDMs can easily be retrofitted into FlexMDMs: on 16 H100s, it takes only three days to fine-tune LLaDA-8B into a FlexMDM, achieving superior performance on math (GSM8K, $58\% \rightarrow 67\%$) and code infilling performance ($52\% \rightarrow 65\%$).

1 Introduction

While diffusion models (Ho et al., 2020; Song et al., 2020; Sohl-Dickstein et al., 2015) are now the leading paradigm for generative modeling in continuous domains, recent work has begun to expand their scope to discrete spaces. The prevailing approach, Masked Diffusion Models (MDMs) (Shi et al., 2024; Sahoo et al., 2024; Gat et al., 2024), generates sentences in a non-left-to-right, any-order fashion. Compared to autoregressive models, this any-order generation ability yields substantially faster inference and strong downstream performance on non-casual tasks such as planning (Ye et al., 2024), code Nie et al. (2025); Ye et al. (2025), and reasoning (Nie et al., 2024).

Despite these successes, current MDMs cannot (1) model distributions supported on sequences of *variable length* and (2) insert new tokens during generation (Figure 1, left). Both capabilities are natural desiderata for generative models over discrete domains. We therefore ask: *Can we model variable-length data while preserving MDMs' any-order generation power?*

We answer in the affirmative by proposing the **Flexible Masked Diffusion Model** (FlexMDM). FlexMDMs start from an empty string and gradually <u>insert mask tokens</u> and then <u>unmask</u> them (Figure 1, right). Beyond learning the usual *unmasking* posterior—the distribution of a clean token at masked positions—we introduce an *insertion* expectation: the expected number of tokens to insert conditioned on the current sequence. Crucially, we show that FlexMDM is theoretically grounded (i.e., under perfect training, it samples from the true data distribution) and retains the anyorder sampling property of MDMs, thereby directly addressing the question above. Empirically, we demonstrate that FlexMDM offers significant new upgrades to the MDM paradigm,

A FlexMDM pretrained on OpenWebText is able to model the length distribution with substantially higher fidelity while matching the perplexity of an MDM counterpart.

¹Harvard University ²Kempner Institute ³Microsoft Research New England

⁴Institute for Artificial Intelligence and Fundamental Interactions, MIT

^{*}equal contribution, randomized ordering; Lee Cheuk-Kit led the theoretical development of the method and engineering effort; Jaeyeon Kim led experiment development and paper presentation. † lead senior authors.

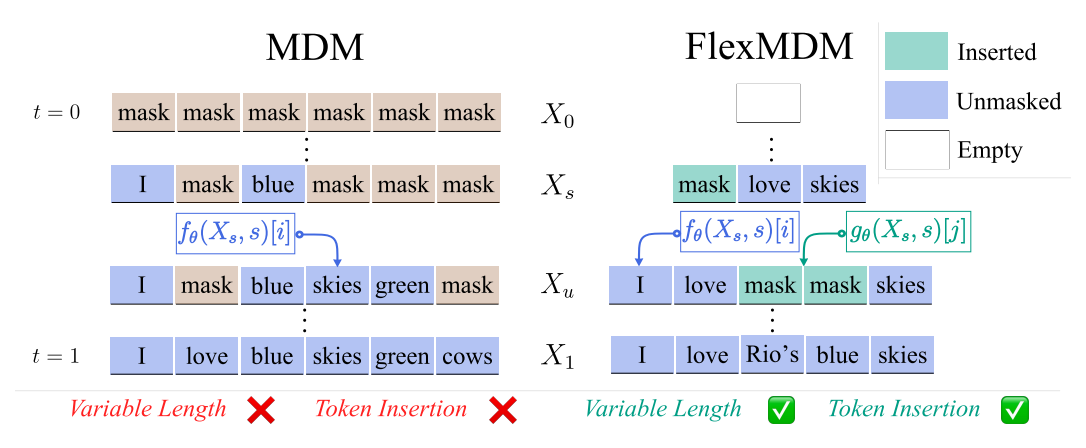


Figure 1: Flexible Masked Diffusion Model (FlexMDM) <u>addresses</u> MDMs' inability to handle variable-length sequences and token insertion while <u>preserving</u> any-order generation power. At each step, FlexMDM performs <u>insertion</u> and <u>unmasking</u> by predicting the expected number of <u>mask tokens to insert</u> (q_{θ}) and the <u>posterior over clean tokens</u> (f_{θ}) , respectively.

- On planning tasks, FlexMDM achieves markedly better results, beating the success rate of MDMs by nearly 60% on a natural synthetic baseline.
- MDMs can be retrofitted into FlexMDMs at 8B+ scale: We fine-tune LLaDA-8B (Nie et al., 2025), an open-source MDM, into a FlexMDM using only 16 H100s for three days. The model transfers cleanly from its MDM initialization and, with its newly acquired variable-length capability, attains notably better performance on GSM8K (58% \rightarrow 67%) and Code infilling (52% \rightarrow 65-%).

Theoretically, our construction relies on the machinery of continuous-time Markov chains (CTMCs) and in particular introduces the new notion of a *joint interpolant*, a novel extension of *stochastic interpolants* (Albergo and Vanden-Eijnden, 2022; Albergo et al., 2023a; Lipman et al., 2022). Recent work (Zheng et al., 2024; Ou et al., 2024) established an equivalence between MDMs and any-order language models—obviating the need for CTMCs. In contrast, we prove that FlexMDMs also possess the flexibility of any-order generation, yet the continuous-time perspective is absolutely essential for them to accurately model the length distribution. Accordingly, we re-derive the connections between MDMs and stochastic interpolants and use them to ground the design of FlexMDMs.

Roadmap. We begin in Section 2 with a broadly accessible review of CTMCs and the connection between MDMs and discrete flow matching. Building on this, Section 3 derives the FlexMDM training objective, and Section 4 introduces our inference procedures. Section 5 presents our experimental results.

Concurrent work. Concurrent works (Wu et al., 2025a; Havasi et al., 2025) attempt to tackle the same problem. Wu et al. (2025a) introduces an auxiliary expand token in training and heuristically replaces each expand token with two mask tokens at inference. Havasi et al. (2025), also based on the discrete flow matching framework, shares a similar theoretical grounding as our result. The main differences lie in our particular choice of interpolant that leads to the development of an any-order sampling algorithm. For clarity, we provide a detailed comparison in Appendix A.

2 PRELIMINARIES: CONTINUOUS-TIME MARKOV CHAINS AND MASKED DIFFUSIONS

In what follows, we provide an overview of continuous-time Markov chains (CTMCs), their role in defining discrete diffusion models, and link them to the MDM framework. As we mentioned in the introduction, this theme is essential to defining FlexMDMs in Section 3.

Transport with continuous-time Markov Chains. Given a target distribution p_1 over sequences with a finite vocabulary set (e.g., text), our aim is to learn to transport samples from a reference distribution p_0 through a continuum of distributions $\{p_t\}_{t\in[0,1]}$ such that $p_{t=1}=p_1$. This type of transport can be realized by a continuous-time Markov chain, which is a stochastic process $\{X_t\}_{t\in[0,1]}$ with $X_0\sim p_0$ governed by a time-dependent transition rate matrix $\{R_t(\cdot,\cdot)\}_{t\in[0,1]}$ satisfying

$$R_t(x,x) = -\sum_{y \neq x} R_t(x,y), \quad R_t(x,y) \ge 0, \ x \ne y.$$
 (1)

Intuitively, the rate matrix determines the infinitesimal likelihood that X_t transitions to any other state y via

$$\mathbb{P}(X_{t+h} = y | X_t = x) = \mathbf{1}_{\{x=y\}} + hR_t(x, y) + o(h),$$
(2)

where we denote the conditional probability measure $\mathbb{P}(\cdot|X_t=x)$ of a new state given the present one. Here o(h) is a remainder term that vanishes faster than h as $h \to 0$. In generative modeling for these discrete distributions, our aims are to (a) specify a path of marginal distributions $\{p_t\}_{t\in[0,1]}$ connecting p_0 to p_1 and (b) learn the associated R_t such that these marginals collectively satisfy the Kolmogorov forward equation:

$$\partial_t p_t(x) = \sum_y p_t(y) R_t(y, x) \qquad p_{t=0} = p_0.$$
 (3)

This ensures that at time t=1, the evolution specified by (2) results in a sample from the target distribution p_1 . The rate matrices defined in this paper are sparse; therefore, we assume that the unspecified entries are 0 and the diagonal entries are defined through Equation (1).

2.1 Masked Diffusion Models

We briefly review MDMs (Sahoo et al., 2024; Shi et al., 2024) and discrete flow matching with the masked construction (Gat et al., 2024), through the lens of stochastic interpolants. The target distribution p_1 assigns probability to length L sequences. The base distribution p_0 employed by these models is the point mass distribution at the fully masked length-L sequence $(\mathbf{m}, \dots, \mathbf{m})$, where \mathbf{m} is an auxiliary mask token.

To define the intermediate $\{p_t\}_{t\in[0,1]}$ that bridges the base and the target, we make use of a stochastic interpolant $\{x_t\}_{t\in[0,1]}$, a collection of random variables whose marginal distribution defines the continuum $\{p_t\}_{t\in[0,1]}$, i.e., $x_t \sim p_t$. Although the previous notion of stochastic interpolant (Albergo et al., 2023a) is defined in a continuous space, it naturally extends to a discrete space, and we defer a formal exposition to Appendix C.

Design of distribution path. The stochastic interpolant relies on a smooth and monotone unmasking schedule $\alpha_t : [0,1] \to [0,1]$ with boundary condition $(\alpha_0, \alpha_1) = (0, 1)$ and time derivative denoted by $\dot{\alpha}_t$. To draw x_t , we first sample a clean sequence $x_1 \sim p_1$; then, independently for every coordinate i, we draw an unmasking time T^i from density $\dot{\alpha}_t dt$ and set

$$x_t^i = \begin{cases} \mathbf{m} & t < T^i \\ x_1^i & t \ge T^i \end{cases}.$$

This process is illustrated in Figure 2. Hence, each equivalently sample the clean sequence $x_1 \sim$ clean token stays masked with probability $1-\alpha_t$ in a p_1 , draw unmasking times, and then accordcoordinate-independent fashion, defining $p_t(\cdot \mid x_1)$. ingly <u>unmask</u> or <u>mask</u> each coordinate's to-We then write p_t by marginalizing over $x_1 \sim p_1$.

MDM Interpolant

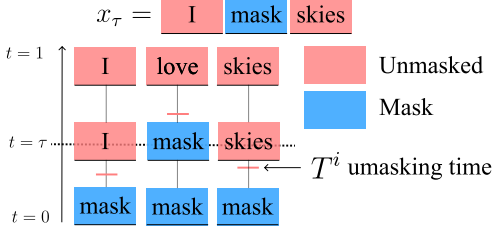


Figure 2: To draw a sample x_t , one can

MDM training. We now derive the MDM rate matrix that induces a CTMC whose marginals coincide with $\{p_t\}_{t\in[0,1]}$ and how it is learned in practice. The central object is the unmasking posterior: the posterior on the clean token x_1^i for masked index i given $x_t = x$ and time step t, i.e., $\mathbb{P}(x_1^i = v | x_t = x)$. We model this posterior with a neural network $f_{\theta}(x,t) \in (\Delta(\Sigma))^n$, where $\Delta(\Sigma)$ denotes a simplex of probability distributions over the vocabulary Σ .

For every position where $x^i = \mathbf{m}$, the network aims to predict $f_{\theta}(x,t)[i,v] \approx \mathbb{P}(x_1^i = v|x_t = x)$, and is trained by minimizing the following variational loss:

$$\mathcal{L}_{\theta} = -\int_{0}^{1} \mathbb{E}\left[\frac{\dot{\alpha}_{t}}{1 - \alpha_{t}} \sum_{i: x_{t}^{i} = \mathbf{m}} \log f_{\theta}(x_{t}, t)[i, x_{1}^{i}]\right] dt. \tag{4}$$

Here, \mathbb{E} denotes the expectation over $x_1 \sim p_1$ and $x_t \sim p_t(\cdot|x_1)$. The minimizer of this loss is the ground-truth unmasking posterior, which fully determines the MDM's rate matrix below. Precisely,

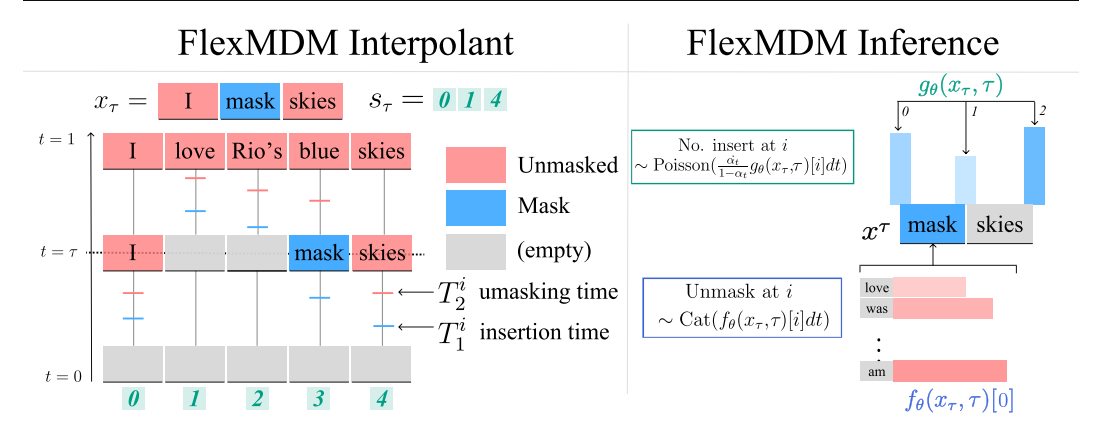


Figure 3: Left (FlexMDM interpolant). To draw a sample x_t , one can equivalently draw a sample $x_1 \sim p_1$, and for each token unmask, mask, or remove it according to the unmasking and insertion times (T_1^i, T_2^i) . An auxiliary interpolant s_t gives closed-form expressions for the FlexMDM rate matrices. Right (FlexMDM Inference). Learned unmasking posterior and insertion expectation are later used at inference.

for $t \in [0,1]$, the rate matrix at time t is given by: for a partially masked sequence $x \in (\Sigma \cup \{\mathbf{m}\})^L$,

$$R_t(x, x[x^i \leftarrow v]) = \frac{\dot{\alpha_t}}{1 - \alpha_t} \underbrace{\mathbb{P}(x_1^i = v | x_t = x)}_{\text{unmasking posterior}}, \quad v \in \Sigma, x^i = \mathbf{m}, \tag{5}$$

where $x[x^i \leftarrow v]$ denotes the sequence obtained from x by replacing its i-th token with v. Therefore, once f_θ has learned the unmasking posterior, one can simulate the CTMC using the rate matrix in (5). The variational loss (4) quantifies the sampling guarantee of this *estimated* CTMC. Let p_1^θ be the terminal distribution of the estimated CTMC. Then, the loss function bounds the KL-divergence:

$$\mathcal{D}_{\mathrm{KL}}(p_1||p_1^{\theta}) \leq \mathcal{L}_{\theta} - \mathcal{L}_{\star},$$

where \mathcal{L}_{\star} is the global minimum of \mathcal{L} . When the loss is in its infimum, the KL divergence vanishes, resulting in the ground truth distribution.

Connections to other MDM frameworks. Connecting to prior works on MDM (Shi et al., 2024; Sahoo et al., 2024; Campbell et al., 2022), defining an interpolant is similar to defining a forward process for the case of diffusion models or a probability path in the case of flow matching. The modeled quantity is identical to the unmasking posterior across all frameworks. For inference, a common scheme is to proceed by: at each intermediate time step, (a) selecting a subset of indices to unmask and (b) sampling clean tokens from the learned posterior. In the infinitesimal limit, this procedure is equivalent to simulating the CTMC of (5). Meanwhile, subsequent work Kim et al. (2025); Nie et al. (2025) shows that MDMs also allow theoretically grounded *any-order inference*: tokens can be unmasked in an arbitrary order without necessarily following the CTMC at (5). We will revisit this aspect in Section 4 and show that our FlexMDM preserves this advantage.

3 Variable Length Masked Diffusions: Training

In this section, we introduce **Flexible Length Masked Diffusion Model** (FlexMDM): a discrete diffusion that models a distribution p_1 assigning probabilities to sequences of different lengths. Following the MDM's recipe, we aim to introduce a stochastic interpolant x_t whose marginal distribution defines the path $\{p_t\}_{t\in[0,1]}$ and learn the corresponding CTMC. Everything hinges on selecting an interpolant that is (a) easy to sample at t=0 and (b) equipped with a closed-form rate matrix amenable to neural network training.

Challenge. Reusing the MDM interpolant is *inadequate*: at t=0, the base distribution p_0 would consist of fully-masked sentences of *variable lengths*, which is impossible to sample since we do not know the length statistics of p_1 in advance. On the other hand, one can consider an interpolant constructed by masking and removing tokens from a clean sequence. However, this *complicates* the rate matrix characterization—token indices shift as insertions occur. To bridge this gap, we introduce the joint interpolant, an extension of the stochastic interpolant that augments the process with an auxiliary variable explicitly tracking token positions. This enlarged state space allows us to construct a broader class of rate matrices while preserving an easy-to-sample base distribution.

Design of distribution path. We now introduce our FlexMDM's joint interpolant that allows us to model the variable length p_1 . This construction relies on *two* smooth, monotone schedules – an insertion schedule $\alpha \colon [0,1] \to [0,1]$ and an unmasking schedule $\beta \colon [0,1] \to [0,1]$, with the boundary conditions $(\alpha_0, \alpha_1) = (\beta_0, \beta_1) = (0,1)$ and time derivatives denoted by $\dot{\alpha}_t, \dot{\beta}_t$.

To draw x_t , we first sample a clean sentence $x_1 \sim p_1$. Independently for each coordinate i, we draw an insertion time T_1^i and an unmasking time T_2^i with $T_1^i < T_2^i$ according to the density below. Accordingly, we either unmask, mask, or remove x_1^i to obtain x_t^i :

$$T_1^i \sim \dot{\alpha_t} \ dt, \qquad T_2^i \sim \mathbf{1}_{\{t \ge T_1^i\}} \frac{\dot{\beta_t}}{1 - \beta_{T_1}} \ dt, \quad x_t^i = \begin{cases} (\text{empty}), & 0 < t < T_1^i \\ \mathbf{m}, & T_1^i \le t < T_2^i \\ x_1^i, & T_2^i \le t \le 1 \end{cases}$$
(6)

Here, 1 denotes the indicator function. We obtain x_t by concatenating the symbols x_t^i , and dropping $x_t^i = \text{(empty)}$. Consequently, the length of x_t is equal to or less than that of x_t^{-1} (see Figure 3, left). As we mentioned above, we augment x_t with an index-tracking variable s_t , forming the joint interpolant (x_t, s_t) . Let $\text{len}(x_t)$ denote the length of x_t ; then

$$s_t$$
: = { $i \in \{0, \dots, \text{len}(x_1) - 1\} \mid T_1^i \le t$ },

i.e., the set of indices whose clean tokens have *not* been deleted. Equivalently, the positions in x_1 referenced by x_t 's each index. By regarding s_t as a list and ordering its elements in ascending order, we also have $x_t = (x_1^{s_t[0]}, \dots, x_1^{s_t[\ln(s_t)-1]})$. We revisit s_t shortly to show how it enables an explicit rate matrix. Since (x_t, s_t) is governed by the sampled unmasking and insertion times, we write $(x_t, s_t) \sim p_t(\cdot \mid x_1)$. Marginalizing $p_t(\cdot \mid x_1)$ over $x_1 \sim p_1$ yields p_t . Since the boundary condition sets $\alpha_0 = \beta_0 = 0$, all tokens are deleted at t = 0; p_0 is the point mass on the empty string.

FlexMDM training. We now explain how we train our FlexMDM to learn the desired rate matrix. We first discuss what the CTMC looks like at a high level: recall from (6) that when *t increases*, tokens are progressively inserted and unmasked. Indeed, one can show that a CTMC that generates the interpolant can be characterized by two quantities that govern the rate of insertion and unmasking:

- Unmasking posterior (modeled by $f_{\theta}(x,t)[i] \in \Delta(\Sigma)$): for each index i that $x^i = \mathbf{m}$, the posterior distribution over the underlying clean token.
- Insertion expectation (modeled by $g_{\theta}(x,t)[i] \in \mathbb{R}_{\geq 0}$): for all indices i in x, the expected number of tokens that remain to be inserted in between x^{i-1} and x^i .

 f_{θ} resembles the familiar unmasking posterior from MDMs, whereas g_{θ} is new: it predicts how many tokens need to be inserted. Intuitively, modeling a *variable-length* p_1 is harder than the fixed-length setup of MDM-introducing an insertion expectation allows us to parameterize more complicated CTMC for FlexMDM; its rate matrix will appear soon in Proposition 2. To define the training loss, we set the boundary values of s_t as $s_t[-1] := -1$ and $s_t[\operatorname{len}(s_t)] := \operatorname{len}(x_1)$, and let $\phi(x,y) = y - x \log y$ denote a scalar Bregman divergence.

$$\mathcal{L}_{\theta} = -\int_{0}^{1} \mathbb{E} \underbrace{\left[\frac{\dot{\beta}_{t}}{1 - \beta_{t}} \sum_{i: \ x_{t}^{i} = \mathbf{m}} \log f_{\theta}(x_{t}, t)[i, x_{1}^{s_{t}[i]}] + \underbrace{\frac{\dot{\alpha}_{t}}{1 - \alpha_{t}} \sum_{i=0}^{\operatorname{len}(x_{t})} \phi(s_{t}[i] - s_{t}[i-1] - 1, g_{\theta}(x_{t}, t)[i])}_{insertion \ loss} \right] dt.}_{insertion \ loss}$$

$$(7)$$

Here, the expectation is taken over $x_1 \sim p_1, (x_t, s_t) \sim p_t(\cdot | x_1)$. Proposition 1 exactly characterizes the unmasking posterior and insertion expectation and shows they uniquely minimize (7).

Proposition 1 (FlexMDM training loss). The loss \mathcal{L}_{θ} in (7) is uniquely minimized at

$$f_{\theta}(x,t)[i,v] = \underbrace{\mathbb{P}(x_1^{s_t[i]} = v | x_t = x)}_{\textit{unmasking posterior}}, \quad g_{\theta}(x,t)[i] = \underbrace{\mathbb{E}[s_t[i] - s_t[i-1] - 1 | x_t = x]}_{\textit{insertion expectation}}.$$

These quantities match the explanation above: the posterior over the clean token together with the expected number of insertions. They precisely determine the FlexMDM rate matrix stated next.

¹Writing x_t^i to mean the symbol derived from source position i is this a mild abuse of notation since the superscript i refers to a position in x_1 rather than a valid index of the (shorter) sequence x_t .

Proposition 2 (FlexMDM Rate Matrix). Let the rate matrix R_t be defined as:

$$\underline{Unmask}: R_t \left(x, x[x^i \leftarrow v] \right) = \frac{\dot{\beta}_t}{1 - \beta_t} \cdot \mathbb{P}(x_1^{s_t[i]} = v | x_t = x), \quad v \in \Sigma, x^i = \mathbf{m}$$

$$\underline{Insert}: R_t \left(x, x \triangleleft_i \mathbf{m} \right) = \frac{\dot{\alpha}_t}{1 - \alpha_t} \cdot \mathbb{E}\left[s_t[i] - s_t[i - 1] - 1 | x_t = x \right], \tag{8}$$

where $x \triangleleft_i \mathbf{m}$ is the sequence obtained from x by inserting a mask token in between (x^{i-1}, x^i) . Then R_t solves the KFE (equation (3)) with p_t as the probability mass function of the FlexMDM interpolant x_t .

Proposition 1 thus implies that minimizing the loss yields exact recovery of the rate matrix. In practice, we could simulate the CTMC using the learned networks (f_{θ}, g_{θ}) in place of the ground-truth quantities in (8). By denoting the resulting terminal distribution as p_1^{θ} , the variational loss quantifies the terminal-time KL divergence:

$$\mathcal{D}_{\mathrm{KL}}(p_1||p_1^{\theta}) \leq \mathcal{L}_{\theta} - \mathcal{L}_{\star}$$

We defer formal demonstration of propositions and the KL divergence guarantee to Appendix D. Definition of the joint interpolant is reinstated in definition D.2, the rate matrix in proposition D.3, the loss and variational bound in proposition D.4.

Remark. Our FlexMDM interpolant introduces only one extra quantity beyond MDM's unmasking posterior: the insertion expectation, a simple scalar per position. This stems from our design choice to gradually insert and then unmask a token. As shown in Section 5.2, this enables efficient task transfer of pretrained MDM weights. In contrast, alternative interpolants would require modeling more complex objects, such as a full token distribution, adding unnecessary training burden.

4 Variable Length Masked Diffusions: Inference

In this section, we outline inference algorithms for FlexMDM, focusing on two variants: **vanilla inference** and **adaptive inference**. We begin with a brief overview of vanilla and adaptive inference in MDMs.

Adaptive inference in MDM. For the case of MDM, MDM inference proceeds by simulating the rate matrix entries in 5. From a high-level one way this can be done is by (a) independently sampling a subset of masked tokens to unmask and (b) sampling clean tokens from the unmasking posterior. Crucially for what follows, the same guarantee holds for non-independent *adaptive* choices of unmasking indices, e.g., confidence-based: correctness hinges on using the ground-truth unmasking posterior, not on following the rate matrix's unmasking entries. This adaptive inference strategy is widely used due to its empirical performance. We adopt this template and show that FlexMDM inherits the same any-order property.

Vanilla inference. We begin with the *vanilla inference* of FlexMDM, which is obtained by discretizing the CTMC in (8) using trained neural networks (f_{θ}, g_{θ}) . Choosing an appropriate discretization scheme is crucial, as different schemes can lead to markedly different empirical behavior. We adopt τ -leaping—originating in chemical physics and shown to outperform naive Euler discretization for MDMs (Campbell et al., 2022)—which batches all events occurring within a fixed interval $[t, t+\tau]$. At a high level, for each discretized step, we simultaneously (Figure 3, right):

- Unmasking: For each mask token, sample for every unmasking a number according to the unmasking intensities in the rate matrix. Unmask only if a non-zero entry is returned.
- Insertion: Sample the number of *mask-token insertions* from a Poisson distribution parameterized by the insertion rate, then apply those insertions.

As the number of steps $\to \infty$, this inference algorithm recovers the CTMC and the discretization error vanishes. Algorithm 1 details the full sampler.

Adaptive inference. Notably, one can choose the positions to unmask adaptively. Precisely, at each inference step we select the unmasking positions according to a heuristic rule that prioritizes the most confident indices, where confidence is computed either from the *model's unmasking posterior* or via a *semi-autoregressive* rule (prioritizing leftmost masks). We find such adaptive choice substantially boosts performance; see Section 5.

Subroutine 2: Unmasking Step Subroutine 1: VLMDM inference **Require:** Learned functions (f_{θ}, g_{θ}) 1: **if** vanilla inference: **Require:** Discretization $0 = t_1 < \cdots < t_N = 1$ 2: for $i \in \{i | X_{t_k}^i = \mathbf{m}\}$ and $v \in \Sigma$ **Require:** Insertion, Unmasking schedule α_t , β_t Set rate $r \leftarrow \frac{\dot{\beta}_{t_k}}{1-\beta_{t_k}} \cdot \tau$ $k_v \sim \operatorname{Poi}(r \cdot f_{\theta}(X_{t_k}, t_k)[i, v])$ if $\exists ! v$ such that $k_v = 1$ 3: 1: Initialize $X_{t_1} \leftarrow \varepsilon$ 4: 2: **for** k = 1 to N - 13: 5: $\tau \leftarrow t_{k+1} - t_k$ 4: **Invoke Subroutine 2 for unmasking** Set $X_{t_k}^i \leftarrow v$ 6: for i in $[\operatorname{len}(X_{t_k})]$ 5: 7: if adaptive inference: Set rate $r \leftarrow \frac{\dot{\alpha}_{t_k}}{1 - \alpha_{t_k}} \cdot \tau$ 6: 8: Select K (the size of |S|) for $i \in \{i | X_{t_k}^i = \mathbf{m}\}$ 9: Sample $\ell \sim \text{Poi}\left(r \cdot g_{\theta}(X_{t_k}, t_k)[i]\right)$ 7: Compute confidence \mathcal{C}^i for i in $\operatorname{argmaxK}(C)$ 10: 8: Insert ℓ masks between $X_{t_k}^{i-1}$ and $X_{t_k}^i$ 11: 9: **return** X_{t_N} $X_{t_k}^i \sim \operatorname{Cat}(f_{\theta}(X_{t_k}, t_k)[i])$ 12:

Algorithm 1: VLMDM inference. At each step we perform unmasking and insertion. For unmasking, unmask by τ -leaping (vanilla) or by confidence-based selection (adaptive). The number of mask tokens to insert is drawn from a Poisson distribution. Notation: Cat, Poi imply the categorical and Poisson distribution, respectively. $\operatorname{argmax} K(\mathcal{C})$ is the indices set of the K largest components of \mathcal{C} . We provide more details in Appendix E.

Since unmasking indices in an adaptive no longer trace the transitions described by the rate matrix entries defined in (8), one might ask whether sampling still guarantees to sample from the target distribution p_1 in the infinitesimal limit. The following proposition answers in the affirmative.

Proposition 3 (Any-order inference, informal). Consider any sampling scheme that, at each step: (i) unmasks an arbitrary subset of masked positions but draws revealed tokens from the ground-truth unmasking posterior; and (ii) applies insertion CTMC governed by the ground-truth rate matrix. Then the resulting process samples from the target distribution p_1 .

The formal statement and the proof of Proposition 3 are given in Appendix E. In words, following the unmasking entries of the rate matrix corresponding to the schedule used in training is *not* necessary to preserve the sampling guarantee. Moreover, the samplers as $N \to \infty$ in Algorithm 1 is subsumed by the class in Proposition 3, therefore, assuming access to the ground-truth unmasking posterior and insertion expectation, the corresponding class of algorithms in Algorithm 1 samples from p_1 up to discretization error.

Remark. A key technical ingredient underlying the rigor of our adaptive inference is that the respective entries of the unmasking posterior of the ground truth rate matrix in Proposition 3 do *not* depend on the choice of unmasking schedule β_t (the proof is given in Appendix E.2.1). This independence allows a single model f_{θ} to learn all possible unmasking transitions arising along different paths that ultimately connect p_0 to p_1 , thereby enabling adaptive unmasking at inference time. This feature is the same mechanism enabling adaptive inference for MDMs, but for FlexMDMs, proving that it interfaces correctly with insertions is quite subtle. Note that a similar notion—independence of the choice of path—has been introduced in continuous spaces Albergo et al. (2023b); Negrel et al. (2025). We defer further discussion to Appendix E.

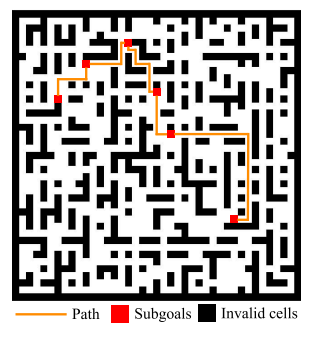
5 EXPERIMENT

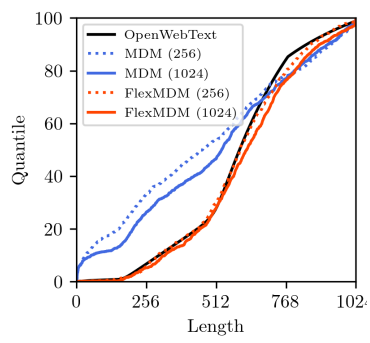
In this section, we present experimental results for FlexMDM, demonstrating the following:

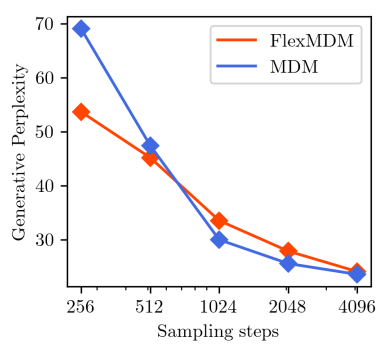
- FlexMDM is an effective variable-length learner: length modeling, planning, local edits.
- FlexMDM is scalable: 8B FlexMDM is obtainable by initializing from a pretrained MDM.

Section 5.1 presents from-scratch results for FlexMDM on text and planning tasks distributions, confirming its practical efficiency. Next, Section 5.2 provides an 8B-scale FlexMDM's training recipe, initialized from LLaDA-8B Nie et al. (2025), and evaluates it in math and code infilling tasks. We begin with the architectural and scheduling choices used throughout.

Training design. Recall from Section 3 that FlexMDM models the unmasking posterior f_{θ} and insertion expectation g_{θ} given state x and time step t. We adopt DiT (Peebles and Xie, 2023), a bidirectional transformer that enables additional embedding, as a backbone. To learn both quantities







(a) Maze task illustration. The model is given subgoals and is required to connect them.

(b) Length modeling. FlexMDM recovers the true length distribution of OpenWebText training data.

(c) Perplexity. FlexMDM achieves generative perplexity on par with MDM.

jointly, we attach two output heads: a standard posterior head for f_{θ} and a scalar softplus head for g_{θ} . Moreover, we choose our unmasking and insertion schedule to be both linear, $\alpha_t = \beta_t = t^2$.

5.1 Pretraining

In this section, we evaluate FlexMDM's ability to learn variable-length data from scratch. Our baseline is MDM, which is fixed-length but can handle variable-length sequences by padding to a fixed maximum length with an auxiliary pad token. This padding setup is widely used in instruction fine-tuning when variable-length answers are desired (Nie et al., 2025; 2024; Ye et al., 2025; Gong et al., 2024). For a fair comparison, we use vanilla inference for both MDM and FlexMDM throughout. Further experimental details appear in Appendix F.

5.1.1 Pretraining on text data

We first construct a training dataset from the raw OpenWebText corpus (Gokaslan et al., 2019), splitting each article into paragraphs to preserve semantic coherence and yield variable-length sequences. Models pretrained on this data, therefore, generate variable-length text.

Results. We train 175M FlexMDM and MDM with a maximum sequence length 1024 for 500K iterations and batch size 1024. Using the pretrained models, we vary the number of sampling steps and measure (a) generative perplexity as a proxy for text fluency, and (b) the induced length distribution. Figure 4c shows comparative generative perplexity for the two models, improving as sampling steps increase, indicating no fluency degradation for FlexMDM despite its more involved loss objective. Crucially, we observe that FlexMDM matches the true length distribution far more closely (Figure 4b): with only 256 steps it tracks the ground truth distribution (red line, whereas MDM remains miscalibrated even at 1024 steps (blue line).

Remark. We remark that our pretraining pipeline differs from prior MDM setups that truncate the corpus to a fixed maximum length. Also, one might ask why we do not provide additional metrics on text benchmarks, such as validation perplexity. This is because MDM and FlexMDM use different objectives (see equation (4) and equation (7)), making likelihood comparisons hard to interpret. We address the concern about the absence of the metric by evaluating scaled models on downstream benchmarks in Section 5.2.

5.1.2 PLANNING TASK

We further evaluate FlexMDM's ability in a planning task in a discrete space. Motivated by an earlier study Janner et al. (2022) that investigated the ability of continuous diffusion in maze tasks, we design a grid-maze benchmark: the maze is fixed but unknown to the model, with a subset of cells invalid. Given a sequence of subgoal grids (g_1, \ldots, g_K) , the model must connect this sequence without entering invalid cells (see Figure 4a). This subgoal structure aligns naturally with FlexMDM: starting from (g_1, \ldots, g_K) , inference inserts mask tokens between subgoals and then unmasks to generate a feasible path. Theoretically, this can be seen as augmenting the base distribution to contain a data-dependent distribution Albergo et al. (2024). This is in stark contrast to MDM, where it

²The ground-truth unmasking posterior is independent of β_t , so we condition the network on α_t only; under the linear choice $\alpha_t = t$, this coincides with the usual time embedding.

must preassign each subgoal to a specific position, which is difficult to know *a priori*. We provide additional details in Appendix F.2.

Results. We use a 41×41 maze and control the task's difficulty via varying the number of subgoals $K \in \{2,7,12\}$. As K increases, MDM performance degrades markedly, while FlexMDM maintains robust success rates, reaching a gap of up to 60% at K=12. These results firmly support FlexMDM as a principled approach for subgoal-based planning, where preallocating token positions is inherently challenging for fixed-length models.

Difficulty	MDM	FlexMDM
Easy	68.4%	92.3%
Medium	29.3%	90.4%
Hard	24.2%	90.0%

Table 1: FlexMDM outperforms MDM on the subgoal-style maze-planning task.

5.2 SCALING UP FLEXMDM

In this section, we address FlexMDM's scalability by scaling it to 8B parameters and observing notable improvements over an MDM baseline. We start from the observation that MDM and FlexMDM both share the unmasking posterior as a core component, suggesting effective *task transfer* from a pretrained MDM might be possible. To demonstrate this, concretely, we initialize from LLaDA-Base (Nie et al., 2025) and make the following modifications: (a) add time-embedding layers and a scalar head to model the insertion expectation; (b) attach LoRA adapters. Altogether, the resulting number of trainable parameters is ≈400M. To cover both natural and mathematical language, we train on the 50:50 mixture of OpenWebText (Gokaslan et al., 2019) and Proof-Pile-2 (Azerbayev et al., 2023). Surprisingly, we observe rapid transfer: within three days on 16 H100 GPUs, the model generates variable-length sentences. We then instruction-fine-tune (IFT) this base FlexMDM to evaluate it on downstream tasks. See Appendix F for more details ³

Results. For comparison, we train FlexMDM and LLaDA-Base from the same number of IFT pairs. For math and code, respectively, we IFT on the GSM8K train split(Cobbe et al. (2021); ≈8000 pairs) and the educational split of opc-sft-stage-2 (Huang et al., 2024) (≈0.1M pairs), for which IFT-ed models are evaluated in the GSM8K test split and HumanEval-infill (single line) (Bavarian et al., 2022) in zero-shot. Sampling is done by confidence-based sampling with a sliding window. Notably, as the number of sampling steps increases, FlexMDM continues to improve, highlighting its strength in reasoning tasks given sufficient compute—whereas the IFT-ed LLaDA's performance remains flat. Although in this experiment we use IFT on task-specific pairs, we expect that training on a much more diverse instruction—answer pairs with sufficient compute will yield a more generalized model.

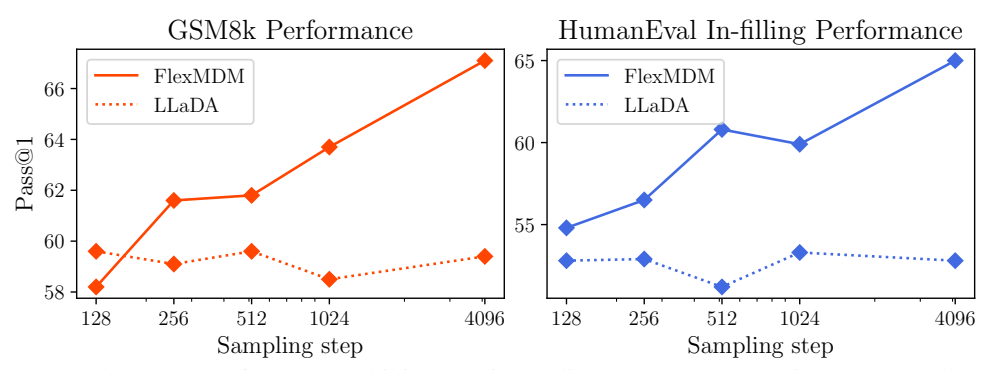


Figure 5: FlexMDM performance exhibits superior scaling when more sampling steps are allocated.

6 Conclusion

In this work we proposed Flexible Masked Diffusion Models (FlexMDM), a discrete diffusion framework over variable-length sequences. Theoretically, via a joint interpolant viewpoint, we provide rigorous guarantees for both training and inference of FlexMDM. Empirically, FlexMDM learns

³For a fair comparison, since FlexMDM is not IFT-ed, we IFT LLaDA-Base, rather LLaDA-instruct, this differs from Zhao et al. (2025). We employ zero-shot evaluation, which also differs from Nie et al. (2024).

variable-length structure across diverse scenarios, scales to 8B parameters, trains in only a few GPU-hours, and yields substantial improvements on math and coding infilling tasks. Further exploration of FlexMDM's capabilities is a promising direction for future work.

Beyond these results, our goal is to align generative modeling with how humans and nature compose discrete sequences. Instead of filling fixed positions; they **insert**, revise, and **reorder** tokens. We hope that our work takes a step in this direction.

ACKNOWLEDGEMENTS

We thank Peter Potaptchik for feedback on the theoretical exposition, Francisco Vargas for discussion on path measures, Jiaxin Shi for discussion on perplexity metrics, Zhenting Qi for discussion on instruction fine-tuning, and Andrew Campbell on architecture of the model. SC is supported by NSF CAREER award CCF-2441635. MSA is supported by a Junior Fellowship at the Harvard Society of Fellows as well as the National Science Foundation under Cooperative Agreement PHY-2019786 (The NSF AI Institute for Artificial Intelligence and Fundamental Interactions, http://iaifi.org/). This work has been made possible in part by a gift from the Chan Zuckerberg Initiative Foundation to establish the Kempner Institute for the Study of Natural and Artificial Intelligence.

REFERENCES

- Jonathan Ho, Ajay Jain, and Pieter Abbeel. Denoising diffusion probabilistic models. *Advances in neural information processing systems*, 33:6840–6851, 2020.
- Yang Song, Jascha Sohl-Dickstein, Diederik P Kingma, Abhishek Kumar, Stefano Ermon, and Ben Poole. Score-based generative modeling through stochastic differential equations. arXiv preprint arXiv:2011.13456, 2020.
- Jascha Sohl-Dickstein, Eric Weiss, Niru Maheswaranathan, and Surya Ganguli. Deep unsupervised learning using nonequilibrium thermodynamics. In *International conference on machine learn*ing, pages 2256–2265. pmlr, 2015.
- Jiaxin Shi, Kehang Han, Zhe Wang, Arnaud Doucet, and Michalis Titsias. Simplified and generalized masked diffusion for discrete data. *Advances in neural information processing systems*, 37: 103131–103167, 2024.
- Subham Sahoo, Marianne Arriola, Yair Schiff, Aaron Gokaslan, Edgar Marroquin, Justin Chiu, Alexander Rush, and Volodymyr Kuleshov. Simple and effective masked diffusion language models. *Advances in Neural Information Processing Systems*, 37:130136–130184, 2024.
- Itai Gat, Tal Remez, Neta Shaul, Felix Kreuk, Ricky TQ Chen, Gabriel Synnaeve, Yossi Adi, and Yaron Lipman. Discrete flow matching. *Advances in Neural Information Processing Systems*, 37: 133345–133385, 2024.
- Jiacheng Ye, Jiahui Gao, Shansan Gong, Lin Zheng, Xin Jiang, Zhenguo Li, and Lingpeng Kong. Beyond autoregression: Discrete diffusion for complex reasoning and planning. arXiv preprint arXiv:2410.14157, 2024.
- Shen Nie, Fengqi Zhu, Zebin You, Xiaolu Zhang, Jingyang Ou, Jun Hu, Jun Zhou, Yankai Lin, Ji-Rong Wen, and Chongxuan Li. Large language diffusion models. *arXiv preprint arXiv:2502.09992*, 2025.
- Jiacheng Ye, Zhihui Xie, Lin Zheng, Jiahui Gao, Zirui Wu, Xin Jiang, Zhenguo Li, and Lingpeng Kong. Dream 7b, 2025. URL https://hkunlp.github.io/blog/2025/dream.
- Shen Nie, Fengqi Zhu, Chao Du, Tianyu Pang, Qian Liu, Guangtao Zeng, Min Lin, and Chongxuan Li. Scaling up masked diffusion models on text. *arXiv preprint arXiv:2410.18514*, 2024.
- Michael S. Albergo and Eric Vanden-Eijnden. Building normalizing flows with stochastic interpolants, 2022.

- Michael S Albergo, Nicholas M Boffi, and Eric Vanden-Eijnden. Stochastic interpolants: A unifying framework for flows and diffusions. *arXiv preprint arXiv:2303.08797*, 2023a.
- Yaron Lipman, Ricky T. Q. Chen, Heli Ben-Hamu, Maximilian Nickel, and Matt Le. Flow matching for generative modeling, 2022.
- Kaiwen Zheng, Yongxin Chen, Hanzi Mao, Ming-Yu Liu, Jun Zhu, and Qinsheng Zhang. Masked diffusion models are secretly time-agnostic masked models and exploit inaccurate categorical sampling. *arXiv preprint arXiv:2409.02908*, 2024.
- Jingyang Ou, Shen Nie, Kaiwen Xue, Fengqi Zhu, Jiacheng Sun, Zhenguo Li, and Chongxuan Li. Your absorbing discrete diffusion secretly models the conditional distributions of clean data. *arXiv preprint arXiv:2406.03736*, 2024.
- Zirui Wu, Lin Zheng, Zhihui Xie, Jiacheng Ye, Jiahui Gao, Yansong Feng, Zhenguo Li, Victoria W., Guorui Zhou, and Lingpeng Kong. Dreamon: Diffusion language models for code infilling beyond fixed-size canvas, 2025a. URL https://hkunlp.github.io/blog/2025/dreamon.
- Marton Havasi, Brian Karrer, Itai Gat, and Ricky TQ Chen. Edit flows: Flow matching with edit operations. *arXiv preprint arXiv:2506.09018*, 2025.
- Andrew Campbell, Joe Benton, Valentin De Bortoli, Thomas Rainforth, George Deligiannidis, and Arnaud Doucet. A continuous time framework for discrete denoising models. *Advances in Neural Information Processing Systems*, 35:28266–28279, 2022.
- Jaeyeon Kim, Kulin Shah, Vasilis Kontonis, Sham Kakade, and Sitan Chen. Train for the worst, plan for the best: Understanding token ordering in masked diffusions. *arXiv* preprint arXiv:2502.06768, 2025.
- Michael S. Albergo, Nicholas M. Boffi, Michael Lindsey, and Eric Vanden-Eijnden. Multimarginal generative modeling with stochastic interpolants, 2023b. URL https://arxiv.org/abs/2310.03695.
- Hugo Negrel, Florentin Coeurdoux, Michael S. Albergo, and Eric Vanden-Eijnden. Multitask learning with stochastic interpolants, 2025. URL https://arxiv.org/abs/2508.04605.
- William Peebles and Saining Xie. Scalable diffusion models with transformers. In *Proceedings of the IEEE/CVF international conference on computer vision*, pages 4195–4205, 2023.
- Shansan Gong, Shivam Agarwal, Yizhe Zhang, Jiacheng Ye, Lin Zheng, Mukai Li, Chenxin An, Peilin Zhao, Wei Bi, Jiawei Han, et al. Scaling diffusion language models via adaptation from autoregressive models. *arXiv preprint arXiv:2410.17891*, 2024.
- Aaron Gokaslan, Vanya Cohen, Ellie Pavlick, and Stefanie Tellex. Openwebtext corpus. http://Skylion007.github.io/OpenWebTextCorpus, 2019.
- Michael Janner, Yilun Du, Joshua Tenenbaum, and Sergey Levine. Planning with diffusion for flexible behavior synthesis. In *International Conference on Machine Learning*, 2022.
- Michael Samuel Albergo, Mark Goldstein, Nicholas Matthew Boffi, Rajesh Ranganath, and Eric Vanden-Eijnden. Stochastic interpolants with data-dependent couplings. In *Forty-first International Conference on Machine Learning*, 2024. URL https://openreview.net/forum?id=FFILRGD0jG.
- Zhangir Azerbayev, Hailey Schoelkopf, Keiran Paster, Marco Dos Santos, Stephen McAleer, Albert Q. Jiang, Jia Deng, Stella Biderman, and Sean Welleck. Llemma: An open language model for mathematics, 2023.
- Siyan Zhao, Devaansh Gupta, Qinqing Zheng, and Aditya Grover. d1: Scaling reasoning in diffusion large language models via reinforcement learning. *arXiv preprint arXiv:2504.12216*, 2025.
- Karl Cobbe, Vineet Kosaraju, Mohammad Bavarian, Mark Chen, Heewoo Jun, Lukasz Kaiser, Matthias Plappert, Jerry Tworek, Jacob Hilton, Reiichiro Nakano, et al. Training verifiers to solve math word problems. *arXiv preprint arXiv:2110.14168*, 2021.

- Siming Huang, Tianhao Cheng, Jason Klein Liu, Jiaran Hao, Liuyihan Song, Yang Xu, J. Yang, J. H. Liu, Chenchen Zhang, Linzheng Chai, Ruifeng Yuan, Zhaoxiang Zhang, Jie Fu, Qian Liu, Ge Zhang, Zili Wang, Yuan Qi, Yinghui Xu, and Wei Chu. Opencoder: The open cookbook for top-tier code large language models. 2024. URL https://arxiv.org/pdf/2411.04905.
- Mohammad Bavarian, Heewoo Jun, Nikolas Tezak, John Schulman, Christine McLeavey, Jerry Tworek, and Mark Chen. Efficient training of language models to fill in the middle. *arXiv* preprint arXiv:2207.14255, 2022.
- Xinyin Ma, Runpeng Yu, Gongfan Fang, and Xinchao Wang. dkv-cache: The cache for diffusion language models. *arXiv preprint arXiv:2505.15781*, 2025a.
- Subham Sekhar Sahoo, Zhihan Yang, Yash Akhauri, Johnna Liu, Deepansha Singh, Zhoujun Cheng, Zhengzhong Liu, Eric Xing, John Thickstun, and Arash Vahdat. Esoteric language models. arXiv preprint arXiv:2506.01928, 2025.
- Chengyue Wu, Hao Zhang, Shuchen Xue, Zhijian Liu, Shizhe Diao, Ligeng Zhu, Ping Luo, Song Han, and Enze Xie. Fast-dllm: Training-free acceleration of diffusion llm by enabling kv cache and parallel decoding. *arXiv preprint arXiv:2505.22618*, 2025b.
- Emiel Hoogeboom, Didrik Nielsen, Priyank Jaini, Patrick Forré, and Max Welling. Argmax flows and multinomial diffusion: Learning categorical distributions. *Advances in neural information processing systems*, 34:12454–12465, 2021.
- Jacob Austin, Daniel D Johnson, Jonathan Ho, Daniel Tarlow, and Rianne Van Den Berg. Structured denoising diffusion models in discrete state-spaces. Advances in neural information processing systems, 34:17981–17993, 2021.
- Aaron Lou, Chenlin Meng, and Stefano Ermon. Discrete diffusion modeling by estimating the ratios of the data distribution. *arXiv preprint arXiv:2310.16834*, 2023.
- Andrew Campbell, Jason Yim, Regina Barzilay, Tom Rainforth, and Tommi Jaakkola. Generative flows on discrete state-spaces: Enabling multimodal flows with applications to protein co-design. arXiv preprint arXiv:2402.04997, 2024.
- Neta Shaul, Itai Gat, Marton Havasi, Daniel Severo, Anuroop Sriram, Peter Holderrieth, Brian Karrer, Yaron Lipman, and Ricky TQ Chen. Flow matching with general discrete paths: A kinetic-optimal perspective. *arXiv* preprint arXiv:2412.03487, 2024.
- Fred Zhangzhi Peng, Zachary Bezemek, Sawan Patel, Jarrid Rector-Brooks, Sherwood Yao, Avishek Joey Bose, Alexander Tong, and Pranam Chatterjee. Path planning for masked diffusion model sampling. *arXiv preprint arXiv:2502.03540*, 2025.
- Litu Rout, Constantine Caramanis, and Sanjay Shakkottai. Anchored diffusion language model. arXiv preprint arXiv:2505.18456, 2025.
- Shansan Gong, Ruixiang Zhang, Huangjie Zheng, Jiatao Gu, Navdeep Jaitly, Lingpeng Kong, and Yizhe Zhang. Diffucoder: Understanding and improving masked diffusion models for code generation. *arXiv preprint arXiv:2506.20639*, 2025.
- Yuxuan Song, Zheng Zhang, Cheng Luo, Pengyang Gao, Fan Xia, Hao Luo, Zheng Li, Yuehang Yang, Hongli Yu, Xingwei Qu, et al. Seed diffusion: A large-scale diffusion language model with high-speed inference. *arXiv preprint arXiv:2508.02193*, 2025.
- Inception Labs, Samar Khanna, Siddhant Kharbanda, Shufan Li, Harshit Varma, Eric Wang, Sawyer Birnbaum, Ziyang Luo, Yanis Miraoui, Akash Palrecha, et al. Mercury: Ultra-fast language models based on diffusion. arXiv preprint arXiv:2506.17298, 2025.
- Heli Ben-Hamu, Itai Gat, Daniel Severo, Niklas Nolte, and Brian Karrer. Accelerated sampling from masked diffusion models via entropy bounded unmasking. arXiv preprint arXiv:2505.24857, 2025.
- Alexander Swerdlow, Mihir Prabhudesai, Siddharth Gandhi, Deepak Pathak, and Katerina Fragkiadaki. Unified multimodal discrete diffusion. *arXiv preprint arXiv:2503.20853*, 2025.

- Google DeepMind. Gemini diffusion, 2025. URL https://blog.google/technology/google-deepmind/gemini-diffusion/.
- Huiwen Chang, Han Zhang, Lu Jiang, Ce Liu, and William T Freeman. Maskgit: Masked generative image transformer. In *Proceedings of the IEEE/CVF conference on computer vision and pattern recognition*, pages 11315–11325, 2022.
- Long Ma, Fangwei Zhong, and Yizhou Wang. Reinforced context order recovery for adaptive reasoning and planning. *arXiv preprint arXiv:2508.13070*, 2025b.
- Zhe Wang, Jiaxin Shi, Nicolas Heess, Arthur Gretton, and Michalis K Titsias. Learning-order autoregressive models with application to molecular graph generation. *arXiv* preprint arXiv:2503.05979, 2025.
- Alec Radford and Jeffrey Wu. Rewon child, david luan, dario amodei, and ilya sutskever. 2019. Language models are unsupervised multitask learners. OpenAI blog, 1(8):9, 2019.
- Juechu Dong, Boyuan Feng, Driss Guessous, Yanbo Liang, and Horace He. Flex attention: A programming model for generating optimized attention kernels. *arXiv preprint arXiv:2412.05496*, 2024.
- Tri Dao, Dan Fu, Stefano Ermon, Atri Rudra, and Christopher Ré. Flashattention: Fast and memory-efficient exact attention with io-awareness. *Advances in neural information processing systems*, 35:16344–16359, 2022.
- Hugo Touvron, Louis Martin, Kevin Stone, Peter Albert, Amjad Almahairi, Yasmine Babaei, Nikolay Bashlykov, Soumya Batra, Prajjwal Bhargava, Shruti Bhosale, Dan Bikel, Lukas Blecher, Cristian Canton Ferrer, Moya Chen, Guillem Cucurull, David Esiobu, Jude Fernandes, Jeremy Fu, Wenyin Fu, Brian Fuller, Cynthia Gao, Vedanuj Goswami, Naman Goyal, Anthony Hartshorn, Saghar Hosseini, Rui Hou, Hakan Inan, Marcin Kardas, Viktor Kerkez, Madian Khabsa, Isabel Kloumann, Artem Korenev, Punit Singh Koura, Marie-Anne Lachaux, Thibaut Lavril, Jenya Lee, Diana Liskovich, Yinghai Lu, Yuning Mao, Xavier Martinet, Todor Mihaylov, Pushkar Mishra, Igor Molybog, Yixin Nie, Andrew Poulton, Jeremy Reizenstein, Rashi Rungta, Kalyan Saladi, Alan Schelten, Ruan Silva, Eric Michael Smith, Ranjan Subramanian, Xiaoqing Ellen Tan, Binh Tang, Ross Taylor, Adina Williams, Jian Xiang Kuan, Puxin Xu, Zheng Yan, Iliyan Zarov, Yuchen Zhang, Angela Fan, Melanie Kambadur, Sharan Narang, Aurelien Rodriguez, Robert Stojnic, Sergey Edunov, and Thomas Scialom. Llama 2: Open foundation and fine-tuned chat models. *arXiv preprint arXiv: 2307.09288*, 2023.
- Ilya Loshchilov and Frank Hutter. Decoupled weight decay regularization. *arXiv preprint* arXiv:1711.05101, 2017.
- Xiao Bi, Deli Chen, Guanting Chen, Shanhuang Chen, Damai Dai, Chengqi Deng, Honghui Ding, Kai Dong, Qiushi Du, Zhe Fu, et al. Deepseek llm: Scaling open-source language models with longtermism. *arXiv preprint arXiv:2401.02954*, 2024.
- Qwen. Qwen2 technical report. arXiv preprint arXiv:2407.10671, 2024.
- Edward J Hu, yelong shen, Phillip Wallis, Zeyuan Allen-Zhu, Yuanzhi Li, Shean Wang, Lu Wang, and Weizhu Chen. LoRA: Low-rank adaptation of large language models. In *International Conference on Learning Representations*, 2022. URL https://openreview.net/forum?id=nZeVKeeFYf9.
- Xingchao Liu, Chengyue Gong, and Qiang Liu. Flow straight and fast: Learning to generate and transfer data with rectified flow, 2022. URL https://arxiv.org/abs/2209.03003.
- Peter Holderrieth, Marton Havasi, Jason Yim, Neta Shaul, Itai Gat, Tommi Jaakkola, Brian Karrer, Ricky T. Q. Chen, and Yaron Lipman. Generator matching: Generative modeling with arbitrary markov processes. In *The Thirteenth International Conference on Learning Representations*, 2025a. URL https://openreview.net/forum?id=RuP17cJtZo.
- Joe Benton, Yuyang Shi, Valentin De Bortoli, George Deligiannidis, and Arnaud Doucet. From denoising diffusions to denoising markov models, 2024. URL https://arxiv.org/abs/2211.03595.

- Andrew Campbell, William Harvey, Christian Weilbach, Valentin De Bortoli, Tom Rainforth, and Arnaud Doucet. Trans-dimensional generative modeling via jump diffusion models, 2023. URL https://arxiv.org/abs/2305.16261.
- Francisco Vargas, Shreyas Padhy, Denis Blessing, and Nikolas Nüsken. Transport meets variational inference: Controlled monte carlo diffusions, 2025. URL https://arxiv.org/abs/2307.01050.
- Julius Berner, Lorenz Richter, and Karen Ullrich. An optimal control perspective on diffusion-based generative modeling. *Transactions on Machine Learning Research*, 2024. ISSN 2835-8856. URL https://openreview.net/forum?id=oYIjw37pTP.
- Stefano Peluchetti. Non-denoising forward-time diffusions, 2022. URL https://openreview.net/forum?id=oVfIKuhqfC.
- Peter Holderrieth, Michael Samuel Albergo, and Tommi Jaakkola. LEAPS: A discrete neural sampler via locally equivariant networks. In *Forty-second International Conference on Machine Learning*, 2025b. URL https://openreview.net/forum?id=Hq2RniQAET.
- Neta Shaul, Itai Gat, Marton Havasi, Daniel Severo, Anuroop Sriram, Peter Holderrieth, Brian Karrer, Yaron Lipman, and Ricky T. Q. Chen. Flow matching with general discrete paths: A kinetic-optimal perspective. In *The Thirteenth International Conference on Learning Representations*, 2025. URL https://openreview.net/forum?id=tcvMzR2NrP.

CONTENTS

1	Introduction		1
2	Preliminaries: Continuous-Time Markov Chains and Masked Diffusions		
	2.1	Masked Diffusion Models	3
3	Vari	able Length Masked Diffusions: Training	4
4	Variable Length Masked Diffusions: Inference		6
5	Experiment		7
	5.1	Pretraining	8
		5.1.1 Pretraining on text data	8
		5.1.2 Planning task	8
	5.2	Scaling up FlexMDM	9
6	Con	onclusion	
A	Rela	elated Works 1	
В	Nota	otation 1	
C	Disc	Discrete Stochastic Interpolants: Definitions and Propositions for Section 2	
	C.1	Discrete Stochastic Interpolant	18
	C.2	The Masked Diffusion Interpolant	19
D	Join	Joint Discrete Stochastic Interpolants: Definitions and Propositions for Section 3	
	D.1	Joint Interpolant	21
	D.2	Flexible-Length Masked Diffusion	22
E	Deta	etails for Section 4	
	E.1	Precise detail on the inference algorithms	25
	E.2	Proof of FlexMDM's any-order inference capability	26
		E.2.1 Proof preliminaries	26
	E.3	Formal guarantee for adaptive inference	26
	E.4	Proof of Theorem E.1	27
	E.5	Proof of Lemma E.1	28
	E.6	Proof of Lemma E.2	28
F	Experimental details		29
	F.1	Pretraining on OpenWebText	29
	F.2	Pretraining on the Maze planning task	30

D	
Pre	print
110	ρ_{1111}

A RELATED WORKS

Discrete diffusion and flows. Early diffusion models were formulated as continuous-time Markov chains over continuous spaces with Gaussian transition kernels (Sohl-Dickstein et al., 2015; Ho et al., 2020), and were later connected to continuous-time formulations via stochastic differential equations, offering a unifying perspective on score-based generative modeling (Song et al., 2020). In parallel, *discrete* diffusion has been developed from the viewpoint of Markov chains over discrete space (Hoogeboom et al., 2021). Notably, Austin et al. (2021) introduced D3PM with several families of discrete transition kernels, and Lou et al. (2023) proposed SEDD, which adopts score-based training objectives. A complementary line of work studies *discrete flows* (Campbell et al., 2024; Gat et al., 2024), aiming to understand continuous-time Markov chains (CTMCs) that interpolate between data and base distributions; this perspective aligns with ours. Subsequent extensions consider token-wise paths and path-wise structure within such flows (Shaul et al., 2024).

Masked Diffusion Models. Among discrete-transition designs, absorbing-state (a.k.a. masking) kernels have become a popular and strong-performing choice. Recent work shows that this yields a simple and principled training recipe, referred to as Masked Diffusion Models (MDMs) (Sahoo et al., 2024; Shi et al., 2024). A growing body of results demonstrates the scalability of this approach across problem settings and modalities, including large-scale natural language modeling (Nie et al., 2024; 2025; Ye et al., 2025; Song et al., 2025; DeepMind, 2025), code generation (Labs et al., 2025; Gong et al., 2025), and multimodal learning (Swerdlow et al., 2025).

Any-order inference in MDMs. With the advent of MDMs, subsequent work has established that they admit theoretically grounded *any-order inference*, wherein tokens can be unmasked in arbitrary orders rather than following a fixed CTMC schedule (Kim et al., 2025; Peng et al., 2025). Practical token-ordering rules span a spectrum of heuristics based on model confidence and uncertainty—e.g., maximum-probability logits (Chang et al., 2022; Zheng et al., 2024), probability margin (Kim et al., 2025), semi-autoregressive schedules (Nie et al., 2024), and entropy-based criteria (Ben-Hamu et al., 2025)—as well as strategies that leverage reference models to guide the unmasking trajectory (Peng et al., 2025). Beyond heuristics, another thread trains auxiliary modules to anchor or adapt the generation order (Rout et al., 2025), while recent work directly *learns* token orders end-to-end (Ma et al., 2025b; Wang et al., 2025).

Stochastic interpolant. Stochastic interpolant (Albergo and Vanden-Eijnden, 2022; Albergo et al., 2023a) is a general framework for building measure-transport based generative models on continuous state space. While building off different philosophical grounds, it can be seen as equivalent to flow matching (Lipman et al., 2022; Liu et al., 2022). Extensions of the interpolant have been proposed for conditional generation through data-dependent coupling (Albergo et al., 2024), which we adopt for infilling task design in Section 5.

Descriptive overview on concurrent work. The most notable concurrent work is Edit-Flow (Havasi et al., 2025), where the primary mathematical machinery that enabled their construction is referred to as "Flow Matching with Auxiliary Process". We note that this can be interpreted as mathematically equivalent to the notion of joint interpolant in this work, e.g., our Proposition D.1 is equivalent to Theorem 3.1 in Havasi et al. (2025).

The main differences are (1) the choice of interpolant and (2) the guarantee of any-order inference. Whereas EditFlow is built around an explicit probability path, we instead define a pair of coupled random variables that implicitly induce this path, leading to a different choice of intermediate. As discussed in Section 3, our choice of interpolant yields a distinct training objective for an unmasking posterior and an insertion-expectation term. Consequently, it enables the any-order inference guarantee established in Section 4.

B NOTATION

In this section, we reiterate the notations used in the main body and introduce auxiliary notations that are used in the proofs of the appendix.

Strings. Let ε denote the empty string, Σ a vocabulary of words, \mathbf{m} a special mask token. We write x^i the i-th element of x with 0-based indexing, $x|_S$ the string indexed by an index set, e.g. $abc[\{0,2\}] = ac$. To insert a token v before position i in string x, we write $x \triangleleft_i v$, e.g., to prepend a token $abc \triangleleft_0 d = dabc$ and to append a token $abc \triangleleft_3 d = abcd$. To replace the i-th token in x with v, we write $x[x^i \leftarrow v]$. As much of the work involves masking, we write $x \subseteq y$ if x can be constructed by partially masking y. We write $\max(x)$, $\max(x) \subseteq [\ln(x)]$ for the set of indices corresponding to mask and clean tokens.

C DISCRETE STOCHASTIC INTERPOLANTS: DEFINITIONS AND PROPOSITIONS FOR SECTION 2

In continuous spaces, a common approach to define generative transport is the stochastic interpolant framework, which implicitly defines the interpolation distribution p_t by specifying an interpolant $\{x_t\}_{t\in[0,1]}$ and regressing the required quantities to realize the transport.

In the section C.1, we introduce a discrete analogue of the stochastic interpolant. To illustrate this framework, we reformulate the widely used masked diffusion model for sequences of length n within our setup. Briefly, masked diffusion defines the interpolation p_t by progressively unmasking tokens in sentences drawn from the data distribution. At time t=0, all tokens are masked, so p_0 is a point mass at the fully masked sequence, the $\mathbf m$ token repeated n times. The transition rates driving the generative transport can be characterized as functions of per-token posterior probabilities conditioned on time t. These are typically learned by minimizing a variational objective in the form of a weighted cross-entropy loss.

C.1 DISCRETE STOCHASTIC INTERPOLANT

To obtain the target rate matrix, the discrete stochastic interpolant relies on an interpolating rate matrix that drives a sample from a sample drawn from a sample from p_0 to a sample from p_1 , defined as follows:

Definition C.1 (Discrete Stochastic Interpolant and Interpolating Rate). Let $x_0 \sim p_0$ and $x_1 \sim p_1$. A discrete stochastic interpolant is a family of random variables $\{x_t\}_{t\in[0,1]}$, defined on a common probability space and satisfying the boundary conditions $x_{t=0} = x_0$ and $x_{t=1} = x_1$, for which there exists a continuous-time Markov chain with bounded, time-dependent transition rate matrix $K_t^{x_0,x_1}$ such that, for each $t\in[0,1]$, Law $(x_t\mid x_0,x_1)$ coincides with the marginal distribution at time t of that Markov chain started at X_0 . We refer to $K_t^{x_0,x_1}$ as an interpolating rate matrix.

With an interpolating rate of an interpolant, the target rate matrix can then be obtained through Proposition C.1

Proposition C.1 (Target Rate). Given a discrete stochastic interpolant x_t and an interpolating rate matrix $K_t^{x_0,x_1}$, the continuous-time Markov chain with initial distribution p_0 and target transition rate matrix R_t defined as,

$$R_t(x,y) = \mathbb{E}_{x_0,x_1}[K_t^{x_0,x_1}(x,y)|x_t=x]$$

has marginals equal to $Law(x_t)$.

Proof. Writing p_t a probability mass function (pmf) of x_t and $p_t(\cdot|x_0,x_1)$ a pmf of x_t conditioned on x_0,x_1 . We further write $q(x_0,x_1)$ the joint pmf of x_0 and x_1 and $q_t(x_0,x_1|x_t)$ to be the joint pmf conditioned on x_t .

It suffices to show R_t satisfies the Kolmogorov Forward Equation with pmf p_t as follows:

$$\sum_{y} R_{t}(y, x) p_{t}(y) = \sum_{y} \mathbb{E}_{x_{0}, x_{1}} [K_{t}^{x_{0}, x_{1}}(x, y) | x_{t} = y] p_{t}(y)$$

$$= \sum_{y} \sum_{x_{0}, x_{1}} K_{t}^{x_{0}, x_{1}}(y, x) q_{t}(x_{0}, x_{1} | y) p_{t}(y)$$

$$= \sum_{y} \sum_{x_{0}, x_{1}} K_{t}^{x_{0}, x_{1}}(y, x) p_{t}(y | x_{0}, x_{1}) q(x_{0}, x_{1})$$

$$= \mathbb{E}_{x_{0}, x_{1}} \left[\sum_{y} K_{t}^{x_{0}, x_{1}}(y, x) p_{t}(y | x_{0}, x_{1}) \right]$$

$$= \mathbb{E}_{x_{0}, x_{1}} \left[\partial_{t} p_{t}(y | x_{0}, x_{1}) \right]$$

$$= \partial_{t} p_{t}(x)$$

This concludes the proof.

Remarks. While written considerably differently, the framework is mathematically equivalent to discrete flow matching Gat et al. (2024). The difference is only philosophical: discrete flow matching relies on the notion of a conditional probability path that the interpolating rate should induce, whereas we define such a probability path only implicitly through the definition of the interpolant.

C.2 THE MASKED DIFFUSION INTERPOLANT

As a concrete example of the discrete stochastic interpolant, we reformulate the masked diffusion model and its learning in the framework. As masked diffusion starts from a point mass, we drop the dependence of x_0 in writing.

Definition C.2 (The Masked Diffusion Interpolant). Let $x_1 \sim p_1$ be a sentence of length n drawn from the data and α_t a smooth unmasking schedule that interpolates from $\alpha_{t=0} = 0$ to $\alpha_{t=1} = 1$. Define the unmasking times $\{T^i\}_{i \in [0,\dots,n-1]}$ as:

$$\forall i \in \{0, \dots, n-1\}: \quad T^i \sim \dot{\alpha}_t \ dt,$$

Then, the masked diffusion interpolant is defined as:

$$x_t = \begin{cases} \mathbf{m} & \text{if } t < T_i, \\ x_1^i & \text{if } t \ge T_i. \end{cases}$$

In other words, at each time t, x_t reveals a subset of the tokens of x_1 , with each token x_1^i independently unmasked at its associated time T^i .

Proposition C.2 (The Masked Diffusion Interpolating Rate). One interpolating rate $K_t^{x_1}$ of the masked diffusion interpolant x_t is given by:

$$\forall x \subseteq x_1, v \in \Sigma, x^i = \mathbf{m} : \quad K_t(x, x[x^i \leftarrow v]) = \frac{\dot{\alpha}_t}{1 - \alpha_t} \mathbf{1}\{v = x_1^i\}.$$

Proof. Let $p_t(\cdot|x_1)$ as the pmf of x_t conditioned on x_1 . From the definition of the interpolant, we notice that:

$$p_t(x|x_1) = \prod_{i=0}^{\text{len}(x_1)-1} \left[(1 - \alpha_t) \mathbf{1} \{ x^i = \mathbf{m} \} + \alpha_t \mathbf{1} \{ x^i = x_1^i \} \right]$$

We verify that K_t satisfies the Kolmogorov Forward Equation (3) under the conditioned pmf as follows,

$$\begin{split} & \text{L.H.S} \\ &= \partial_t p_t(x|x_1) \\ &= \partial_t \left[\prod_{i=0}^{\text{len}(x_1)-1} (1-\alpha_t) \mathbf{1}\{x^i = \mathbf{m}\} + \alpha_t \mathbf{1}\{x^i = x_1^i\} \right] \\ &= \sum_{i=0}^{\text{len}(x_1)-1} \left(-\dot{\alpha}_t \mathbf{1}\{x^i = \mathbf{m}\} + \dot{\alpha}_t \mathbf{1}\{x^i = x_1^i\} \right) \cdot \prod_{j \neq i} (1-\alpha_t) \mathbf{1}\{x^j = \mathbf{m}\} + \alpha_t \mathbf{1}\{x^j = x_j^i\}, \\ &\text{R.H.S} \\ &= \sum_{i=0}^{\text{len}(x_t)-1} \mathbf{1}\{x^i = x_1^i\} \frac{\dot{\alpha}_t}{1-\alpha_t} p_t(x[x^i \leftarrow \mathbf{m}]|x_1) - \mathbf{1}\{x^i = \mathbf{m}\} \frac{\dot{\alpha}_t}{1-\alpha_t} p_t(x|x_1) \\ &= \sum_{i=0}^{\text{len}(x_t)-1} \mathbf{1}\{x^i = x_1^i\} \frac{\dot{\alpha}_t}{1-\alpha_t} (1-\alpha_t) \prod_{j \neq i} (1-\alpha_t) \mathbf{1}\{x^j = \mathbf{m}\} + \alpha_t \mathbf{1}\{x^j = x_j^i\} \\ &- \sum_{i=0}^{\text{len}(x_t)-1} \mathbf{1}\{x^i = \mathbf{m}\} \frac{\dot{\alpha}_t}{1-\alpha_t} (1-\alpha_t) \prod_j (1-\alpha_t) \mathbf{1}\{x^j = \mathbf{m}\} + \alpha_t \mathbf{1}\{x^j = x_j^i\}) \\ &= \text{L.H.S.} \end{split}$$

This concludes the proof.

Note that since each T^i is sampled independently from a continuous distribution, the probability that two unmasking times coincide is zero. Thus, only a single token is unmasked in any infinitesimal transition almost surely.

Proposition 4 (The Masked Diffusion Target Rate). *By proposition C.1, a target rate* R_t *that induces* $Law(x_t)$ *is:*

$$\forall x \subseteq x_1, v \in \Sigma, x^i = \mathbf{m} : \quad R_t(x, x[x^i \leftarrow v]) = \frac{\dot{\alpha}_t}{1 - \alpha_t} \mathbb{P}(x_1^i = v | x_t = x).$$

Proof. Following proposition C.2, the result follows from invoking proposition C.1. \Box

To learn an approximation to R_t , we now parameterize an approximate target rate of the form $\hat{R}_t(x, x[x^i \leftarrow v]) := \frac{\dot{\alpha}_t}{1-\alpha_t} f_{\theta}(x,t)[i,v]$ where $f_{\theta}(x,t)[i,v]$ is a learned approximation to the posterior $\mathbb{P}(x_1^i = v \mid x_t = x)$.

The target rate can then be characterized by a variational objective that measures the discrepancy between the true and approximate path measures.

Proposition 5 (Variational Loss for Masked Diffusion). The loss function is defined as:

$$L[\hat{R}_t] = \int_0^1 \mathbb{E}_{x_1, x_t} \left[-\frac{\dot{\alpha}_t}{1 - \alpha_t} \sum_{i=0}^{n-1} \mathbf{1} \{ x_t^i = \mathbf{m} \} \log f_{\theta}(x_t, t)[i, x_1^i] \right] dt,$$

is uniquely minimized when $\hat{R}_t = R_t$, and is connected to the terminal KL-divergence by:

$$\mathcal{D}_{KL}(p_1||\hat{p}_1) \le L[\hat{R}_t] - L[R_t],$$

where \hat{p}_1 is the approximate data distribution generated by \hat{R}_t .

Proof. Let \mathbb{P} and $\hat{\mathbb{P}}$ be the path measures associated with the continuous-time Markov chain of the target rate matrix R_t in proposition C.1 and an approximation through a neural network \hat{R}_t . The

variational loss follows by expanding the KL-divergence between the two path measures.

$$\mathcal{D}_{\mathrm{KL}}(\mathbb{P} \mid\mid \hat{\mathbb{P}}) = \mathbb{E}_{\mathbb{P}} \left[\int_{t=0}^{t=1} R_{t}(x_{t}, x_{t}) - \hat{R}_{t}(x_{t}, x_{t}) \, dt + \sum_{t: x_{t} \neq x_{t-}} \log \frac{R_{t}(x_{t-}, x_{t})}{\hat{R}_{t}(x_{t-}, x_{t})} \right]$$

$$= \int_{0}^{t=1} \mathbb{E}_{x_{t} \sim \mathbb{P}_{t}} \left[\sum_{y \neq x_{t}} \hat{R}_{t}(x_{t}, y) - R_{t}(x_{t}, y) \log \hat{R}_{t}(x_{t}, y) \right] dt + \mathrm{Const.}$$

$$= \int_{0}^{1} \mathbb{E}_{x_{1}, x_{t}} \left[-\frac{\dot{\alpha}_{t}}{1 - \alpha_{t}} \sum_{i=0}^{n-1} \mathbf{1} \{x_{t}^{i} = \mathbf{m}\} \log f_{\theta}(x_{t}, t)[i, x_{1}^{i}] \right] dt + \mathrm{Const.}$$

where the first line takes the expectation of the Radon-Nikodym derivative between the two path measures. The statement of Radon-Nikodym derivative between two CTMCs can be found in the Appendix in Campbell et al. (2024). A discrete-time equivalent derivation can also be found in Shaul et al. (2025).

The terminal KL bound then follows directly from the data processing inequality, that is:

$$\mathcal{D}_{\mathrm{KL}}(p_1 \mid\mid \hat{p}_1) \leq \mathcal{D}_{\mathrm{KL}}(\mathbb{P}|\mid \hat{\mathbb{P}})$$

This technique is standard, as shown in Vargas et al. (2025) for the case of path reversal-based construction of diffusion generative models, and in Holderrieth et al. (2025b) for discrete diffusion.

D JOINT DISCRETE STOCHASTIC INTERPOLANTS: DEFINITIONS AND PROPOSITIONS FOR SECTION 3

Building on the discrete stochastic interpolant, we proceed to construct a discrete diffusion that models a probability distribution whose supports span variable-length sequences.

On a high level, we would like to define an interpolant constructed by deleting and masking sentences from the data distribution. However, the corresponding interpolating rate becomes cumbersome to characterize, as it is no longer clear what each mask token should unmask to.

To this end, we introduce the **joint interpolant** that allows us to construct a broader class of interpolants and interpolating rate matrices by augmenting the interpolant with auxiliary information that allows us to specify a more flexible interpolation path. We then leverage this newfound freedom to construct the flexible-length masked diffusion model.

D.1 JOINT INTERPOLANT

By introducing an auxiliary variable coupled with the interpolant, the joint interpolant expands the class of interpolating rates that can be defined.

Definition D.1 (Joint Interpolant and Joint Interpolating Rate). Let $x_0 \sim p_0$ and $x_1 \sim p_1$. A **joint interpolant** is a family of coupled random variables $\{(x_t, s_t)\}_{t \in [0,1]}$ defined on a common probability space and satisfying the boundary conditions $x_{t=0} = x_0$ and $x_{t=1} = x_1$, for which there exists a continuous-time Markov chain with bounded, time-dependent transition rate matrix $K_t^{x_0, x_1}$ on the joint state space such that, for each $t \in [0,1]$, the conditional law $\text{Law}(x_t, s_t \mid x_0, x_1)$ coincides with the marginal distribution at time t of this Markov chain started at (x_0, s_0) . We call $K_t^{x_0, x_1}$ a **joint interpolating rate matrix**.

Proposition D.1 (Joint Interpolant Target Rate). Let $\{(x_t, s_t)\}_{t \in [0,1]}$ be a joint interpolant with joint interpolating rate matrix $K_t^{x_0,x_1}$. Consider the continuous-time Markov chain with initial distribution p_0 and target transition rate matrix R_t defined by

$$R_t(x,y) = \mathbb{E}_{s_t,x_0,x_1} \left[\sum_{s' \in \mathcal{S}} K_t^{x_0,x_1} ((x,s_t),(y,s')) \mid x_t = x \right],$$

where S denotes the discrete state space of the auxiliary variable s_t . The marginal of the chain at time t is then equal to Law (x_t) .

We note that this result is equivalent to "Flow Matching with Auxiliary Process" in concurrent work Havasi et al. (2025).

Proof. Let $p_t(\cdot, \cdot|x_0, x_1)$ the joint pmf of x_t , s_t conditioned on x_0, x_1 , let $q_t(x_0, x_1, s_t|x_t)$ to be the joint of x_0, x_1, s_t conditioned on x_t , and let $q_t(x_0, x_1)$ to be the joint of x_0, x_1 . We proceed to verify R_t satisfies the KFE as in Equation 3,

$$\sum_{y} R_{t}(y, x) p_{t}(y) = \sum_{y} \mathbb{E}_{s_{t}, x_{0}, x_{1}} \left[\sum_{s' \in \mathcal{S}} K_{t}^{x_{0}, x_{1}} \left((y, s_{t}), (x, s') \right) \mid x_{t} = y \right] p_{t}(y)$$

$$= \sum_{y} \sum_{s_{t}, x_{0}, x_{1}} \sum_{s' \in \mathcal{S}} K_{t}^{x_{0}, x_{1}} \left((y, s_{t}), (x, s') \right) q_{t}(x_{0}, x_{1}, s_{t} \mid y) p_{t}(y)$$

$$= \sum_{y} \sum_{s_{t}, x_{0}, x_{1}} \sum_{s' \in \mathcal{S}} K_{t}^{x_{0}, x_{1}} \left((y, s_{t}), (x, s') \right) q_{t}(x_{0}, x_{1}, s_{t} \mid y) p_{t}(y)$$

$$= \sum_{y} \sum_{s_{t}, x_{0}, x_{1}} \sum_{s' \in \mathcal{S}} K_{t}^{x_{0}, x_{1}} \left((y, s_{t}), (x, s') \right) p_{t}(y, s_{t} \mid x_{0}, x_{1}) q(x_{0}, x_{1})$$

$$= \mathbb{E}_{x_{0}, x_{1}} \left[\sum_{s'} \partial_{t} p_{t}(x, s' \mid x_{0}, x_{1}) \right]$$

$$= \partial_{t} p_{t}(x \mid x_{0}, x_{1})$$

This concludes the proof.

D.2 FLEXIBLE-LENGTH MASKED DIFFUSION

We then instantiate the joint interpolant to obtain the length-aware masked diffusion model, using a sorted list of indices that has been inserted. Again, we drop x_0 in the writing as the model interpolates between a point mass at an empty sentence to the full data distribution. We redefine the interpolant in equation 6 for clarity.

Definition D.2 (Flexible-Length Masked Diffusion Joint Interpolant). Let $x_1 = (x_1^0, \dots, x_1^{n-1}) \sim p_1$ be a sequence of length n. Let α_t and β_t be monotone and differentiable schedules on [0,1] such that $\alpha_0 = \beta_0 = 0$ and $\alpha_1 = \beta_1 = 1$. Define insertion and unmasking times $\{T_1^i\}_{i=0}^{n-1}$, $\{T_2^i\}_{i=0}^{n-1}$ as follows:

$$\begin{split} T_1^i &\sim \dot{\alpha}_t \ dt, \\ T_2^i &\sim \mathbf{1}\{t \geq T_1^i\} \cdot \frac{\dot{\beta}_t}{1-\beta_{T^i}} \ dt. \end{split}$$

At each time $t \in [0,1]$, define the sorted index set s_t as:

$$s_t = \{i \in \{0, \dots, n-1\} \mid t > T_1^i\},\$$

with ascending order $s_t[0] < \cdots < s_t[\operatorname{len}(s_t) - 1]$, and boundary values:

$$s_t[-1] = -1, \quad s_t[len(s_t)] = n,$$

and define the interpolant state x_t per-coordinate as:

$$x_t^i = \begin{cases} \mathbf{m} & \text{if } t < T_2^{s_t[i]}, \\ x_1^{s_t[i]} & \text{if } t \ge T_2^{s_t[i]}. \end{cases}$$

The process $(s_t, x_t)_{t \in [0,1]}$ is the flexible length masked diffusion joint interpolant.

Here, s_t tracks the ordered set of indices whose tokens have been inserted. The interpolant x_t reveals the true token x_1^i only after both insertion and unmasking. Given access to this ordered set, one interpolating rate is:

Proposition D.2 (FlexMDM Interpolating Rate). A joint interpolating rate matrix $Q_t^{x_0,x_1}$ for the joint interpolant above is given by:

1. Unmask: For index set s, $x \subseteq x_1|_s$, $x^i = \mathbf{m}$, and $v \in \Sigma$:

$$Q_t^{x_1}((x,s), (x[x^i \leftarrow v], s)) = \frac{\dot{\beta}_t}{1 - \beta_t} \cdot \mathbf{1}\{x_1^{s[i]} = v\}$$

2. Insert: For index set s, $x \subseteq x_1|_s$, $j \notin s$, and position i such that s[i-1] < j < s[i]:

$$Q_t^{x_1}((x,s),(x \triangleleft_i \mathbf{m}, s \cup \{j\})) = \frac{\dot{\alpha}_t}{1 - \alpha_t}$$

Proof. We first write down the $p_t(\cdot,\cdot|x_1)$ the conditioned pmf of (s,x) given x_0,x_1 . Let $n=\text{len}(x_t)$, then

$$\begin{split} p_t(s,x \mid x_1) &= A(t) \prod_{i \in s_t} I_i(t), \\ A(t) &:= (1 - \alpha_t)^{n - |s|} \\ I_i(t) &:= \int_0^t \dot{\alpha}_u \left(\frac{1 - \beta_t}{1 - \beta_u} \mathbf{1} \{ x^i = \mathbf{m} \} + \frac{\beta_t - \beta_u}{1 - \beta_u} \mathbf{1} \{ x^i = x_1^i \} \right) du. \end{split}$$

Differentiate using the product rule:

$$\partial_t p_t(s,x\mid x_1) = \dot{A}(t) \prod_{i\in s} I_i(t) + A(t) \sum_{j\in s} \Big(\dot{I}_j(t) \prod_{i\in s\setminus \{j\}} I_i(t)\Big).$$

For $A(t) = (1 - \alpha_t)^{|n-s|}$ we have

$$\dot{A}(t) = -(n - |s|)\dot{\alpha}_t (1 - \alpha_t)^{n - |s| - 1} = A(t) \left(-\frac{(n - |s|)\dot{\alpha}_t}{1 - \alpha_t} \right).$$

For each $i \in s$ apply the Leibniz rule to $I_i(t)$:

$$\dot{I}_{i}(t) = \dot{\alpha}_{t} \mathbf{1} \{x^{i} = \mathbf{m}\} + \int_{0}^{t} \dot{\alpha}_{u} \left(\frac{-\dot{\beta}_{t}}{1 - \beta_{u}} \mathbf{1} \{x^{i} = \mathbf{m}\} + \frac{\dot{\beta}_{t}}{1 - \beta_{u}} \mathbf{1} \{x^{i} = x_{1}^{i}\} \right) du$$

$$= \dot{\alpha}_{t} \mathbf{1} \{x^{i} = \mathbf{m}\} + \dot{\beta}_{t} \left(-\mathbf{1} \{x^{i} = \mathbf{m}\} + \mathbf{1} \{x^{i} = x_{1}^{i}\} \right) \int_{0}^{t} \frac{\dot{\alpha}_{u}}{1 - \beta_{u}} du.$$

Substituting $\dot{A}(t)$ and $\dot{I}_i(t)$ into the product-rule expansion yields

$$\begin{split} &\partial_t p_t(s,x\mid x_1)\\ &= -(n-|s|)\dot{\alpha}_t(1-\alpha_t)^{|n-|s|-1}\prod_{i\in s}I_i(t)\\ &+ (1-\alpha_t)^{|n-|s|}\sum_{j\in s}\left[\left(\dot{\alpha}_t\mathbf{1}\{x^j=\mathbf{m}\} + \dot{\beta}_t\left(-\mathbf{1}\{x^j=\mathbf{m}\} + \mathbf{1}\{x^j=x_1^j\}\right)\int_0^t\frac{\dot{\alpha}_u}{1-\beta_u}\,du\right)\right.\\ &\left. \cdot \prod_{i\in s\setminus\{j\}}I_i(t)\right]\\ &= -(n-|s|)\frac{\dot{\alpha}_t}{1-\alpha_t}A(t)\prod_{i\in s}I_i(t) - \sum_{j\in s,x^j=\mathbf{m}}\frac{\dot{\beta}_t}{1-\beta_t}A(t)\prod_{i\in s}I_i(t)\\ &+ \sum_{j\notin s,x^k\neq\mathbf{m}}\frac{\dot{\beta}_t}{1-\beta_t}A(t)(\int_0^t\dot{\alpha}_u\frac{1-\beta_t}{1-\beta_u}du)\prod_{i\in s-\{j\}}I_i(t) + \sum_{i\in s}\frac{\dot{\alpha}_t}{1-\alpha_t}(1-\alpha_t)A(t)\prod_{i\in s-\{j\}}I_i(t) \end{split}$$

This can then be rewritten term by term as,

$$\begin{split} \partial_t p_t(s,x\mid x_1) &= -\sum_{i\notin s} \frac{\dot{\alpha_t}}{1-\alpha_t} p_t(s,x\mid x_1) - \sum_{x^i = \mathbf{m}} \frac{\dot{\beta_t}}{1-\beta_t} p_t(s,x\mid x_1) \\ &+ \sum_{x^i \neq \mathbf{m}} \frac{\dot{\beta_t}}{1-\beta_t} p_t(s,x[x^i \leftarrow \mathbf{m}]|x_1) + \sum_{x^i = \mathbf{m}} \frac{\dot{\alpha_t}}{1-\alpha_t} p_t(s-\{s[i]\}, \text{remove}(x,i)\mid x_1) \end{split}$$

where remove(x, i) refers to the string constructed by removing the *i*-th element of x.

Notice that this is equivalent to the R.H.S of the KFE (Eq. 3) if one uses the rate matrix $Q_t^{x_1}$. The four terms correspond to 1) Outgoing mass from insertion; 2) Outgoing mass from unmasking; 3) Incoming mass from unmasking; 4) Incoming mass from insertion. This concludes the proof.

Proposition D.3 (FlexMDM Rate Matrix (Restated from Proposition 2)). By Proposition D.1, the induced marginal target rate R_t is:

1. Unmask: For $x^i = \mathbf{m}, v \in \Sigma$:

$$R_t(x, x[x^i \leftarrow v]) = \frac{\dot{\beta}_t}{1 - \beta_t} \cdot \mathbb{P}(x_1^{s_t[i]} = v \mid x_t = x)$$

2. Insert: For position $i \in \{0, ..., |x|\}$:

$$R_t(x, x \triangleleft_i \mathbf{m}) = \frac{\dot{\alpha}_t}{1 - \alpha_t} \cdot \mathbb{E}_{s_t} \left[s_t[i] - s_t[i-1] - 1 \mid x_t = x \right]$$

Proof. The proof follows by noting proposition D.2 and invoking proposition D.1. \Box

Performing an approximate target rate matrix \hat{R}_t in terms of an approximate posterior by token $f_{\theta}(x,t)[i,v] \approx \mathbb{P}(x_1^{s_t[i]} = v \mid x_t = x)$ and an approximate number of insertions $g_{\theta}(x,t)[i] \approx \mathbb{E}_{s_t}\left[s_t[i] - s_t[i-1] - 1 \mid x_t = x\right]$. The target rate matrix can be learned by minimizing the following variational objective. Note that the variational loss objective below is the same as one we defined in equation 7.

Proposition D.4 (FlexMDM Loss (Restated from Proposition 1)). The loss function is defined as:

$$L[\hat{R}_t] = \int_0^1 \mathbb{E}_{x_1, s_t, x_t} \left[-\frac{\dot{\beta}_t}{1 - \beta_t} \sum_{i=0}^{\ln(x_t) - 1} \mathbf{1} \{ x_t^i = \mathbf{m} \} \log f_{\theta}(x_t, t) [i, x_1^{s_t[i]}] \right] dt,$$
$$+ \int_0^1 \mathbb{E}_{x_1, s_t, x_t} \left[\frac{\dot{\alpha}_t}{1 - \alpha_t} \sum_{i=0}^{|x_1|} \phi(s_t[i] - s_t[i-1] - 1, g_{\theta}(x_t, t)[i]) \right] dt,$$

where $\phi(x,y) = y - x \log y$, is uniquely minimized when $\hat{R}_t = R_t$ and is connected by terminal KL-divergence by:

$$\mathcal{D}_{KL}(p_1||\hat{p}_1) \le L[\hat{R}_t] - L[R_t],$$

where \hat{p}_1 is the approximate data distribution induced by \hat{R}_t .

Proof. Let \mathbb{P} and $\hat{\mathbb{P}}$ be the path measure of a continuous time Markov chain starting with the empty string with rate matrix R_t and \hat{R}_t , respectively.

Consider the KL-divergence between path measures \mathbb{P} and $\hat{\mathbb{P}}$,

$$\mathcal{D}_{\mathrm{KL}}(\mathbb{P} \mid\mid \hat{\mathbb{P}}) = \mathbb{E}_{\mathbb{P}} \left[\int_{t=0}^{t=1} R_{t}(x_{t}, x_{t}) - \hat{R}_{t}(x_{t}, x_{t}) \, dt + \sum_{t: x_{t} \neq x_{t-}} \log \frac{R_{t}(x_{t-}, x_{t})}{\hat{R}_{t}(x_{t-}, x_{t})} \right]$$

$$= \int_{0}^{t=1} \mathbb{E}_{x_{t}} \left[\sum_{y \neq x_{t}} \hat{R}_{t}(x_{t}, y) - R_{t}(x_{t}, y) \log \hat{R}_{t}(x_{t}, y) \right] dt + \text{Const.}$$

$$= \int_{0}^{t=1} \mathbb{E}_{x_{t}} \left[\sum_{y \neq x_{t}} \hat{R}_{t}(x_{t}, y) - R_{t}(x_{t}, y) \log \hat{R}_{t}(x_{t}, y) \right] dt + \text{Const.}$$

$$= \int_{0}^{1} \mathbb{E}_{x_{1}, s_{t}, x_{t}} \left[-\frac{\dot{\beta}_{t}}{1 - \beta_{t}} \sum_{i=0}^{\ln(x_{t}) - 1} \mathbf{1} \{x_{t}^{i} = \mathbf{m}\} \log f_{\theta}(x_{t}, t)[i, x_{1}^{s_{t}[i]}] \right] dt$$

$$+ \int_{0}^{1} \mathbb{E}_{x_{1}, s_{t}, x_{t}} \left[\frac{\dot{\alpha}_{t}}{1 - \alpha_{t}} \sum_{i=0}^{|x_{1}|} \phi(s_{t}[i] - s_{t}[i-1] - 1, g_{\theta}(x_{t}, t)[i]) \right] dt + \text{Const.}$$

The terminal KL-bound then follows from the data processing inequality, that is:

$$\mathcal{D}_{\mathrm{KL}}(p_1||\hat{p}_1) \leq \mathcal{D}_{\mathrm{KL}}(\mathbb{P}||\hat{\mathbb{P}})$$

E DETAILS FOR SECTION 4

E.1 Precise detail on the inference algorithms

In this section, we provide details on the unmasking steps of vanilla and adaptive inference for FlexMDM, summarized in Algorithm 1, Subroutine 2. Suppose at inference time we are given the discretization step size τ , a partially observed sequence X_{t_k} , and the current time step t_k .

Vanilla inference. For each masked position i (i.e., $X_{t_k}^i = \mathbf{m}$) and each clean token $v \in \Sigma$, we sample unmasking events from a Poisson distribution $\operatorname{Poisson}(R_v\tau)$, where R_v is the unmasking rate toward token v. Concretely, $R_v = \frac{\dot{\beta}_{t_k}}{1-\beta_{t_k}} \cdot f_{\theta}(X_{t_k}, t_k)[i, v]$, so that the event count is distributed as $k_v \sim \operatorname{Poi}\left(\tau \cdot \frac{\dot{\beta}_{t_k}}{1-\beta_{t_k}} \cdot f_{\theta}(X_{t_k}, t_k)[i, v]\right)$. A masked position is unmasked only if exactly one token v produces a count $k_v = 1$ while all others produce zero. This tau-leaping scheme batches all events that occur within the interval $[t_k, t_k + \tau]$.

Adaptive inference. We first draw the number of tokens to unmask, denoted by an integer K. While Proposition 3 (Theorem E.1) shows that the choice of K does not affect the theoretical guarantees, in practice, we set K to match the expected number of unmasked tokens under vanilla inference yields stable behavior. Accordingly, we sample $K \sim \operatorname{Poi}\left(\tau \cdot \frac{\dot{\beta}_{t_k}}{1-\dot{\beta}_{t_k}} \cdot \#\{\text{masked tokens in } X_{t_k}\}\right)$.

Next, we compute a confidence score for each masked position, based on heuristics such as:

- Top-K probability (Chang et al., 2022; Zheng et al., 2024): For state x at time t, the confidence at position i is given by $\max_{v \in \Sigma} f_{\theta}(x, t)[i, v]$.
- Top-K probability with sliding window: We further restrict sampling to the leftmost L tokens, where

$$L = \min(|\gamma_1 \cdot L|, \gamma_2),$$

with γ_1 and γ_2 hyperparameters. This approach is related to semi-autoregressive strategies used in Nie et al. (2025).

Finally, we select the subset of positions to unmask as the Top-K masked indices with the highest confidence scores.

E.2 Proof of FlexMDM's any-order inference capability

E.2.1 PROOF PRELIMINARIES

Form of posterior. We first compute, for each x_i^t , the probabilities of being masked or deleted in equation (6). This follows from a straightforward calculation using the joint distribution of (T_1^i, T_2^i) :

$$\begin{split} p(x_t^i = (\text{empty})) &= p(T_1^i > t) = 1 - \alpha_t, \\ p(x_t^i = \mathbf{m}) &= p(T_1^i \leq t, T_2^i > t) = \int_t^1 \int_0^t \left(\frac{\dot{\beta}_s}{1 - \beta_u} \times \dot{\alpha}_s\right) ds du = :1 - \gamma_t. \end{split}$$

Here we define γ_t as $1-p(x_t^i=\mathbf{m})$. Therefore, the process in equation (6) is equivalent to observing a partially masked subsequence x_t obtained by sampling $x_1 \sim p$ and, for each position of x_1 , independently deleting it with probability $1-\alpha_t$, masking it with probability $1-\gamma_t$, or leaving it unchanged with probability $\alpha_t + \gamma_t - 1$. Note that α_t and γ_t both increase from 0 to 1 as t increases from 0 to 1.

The posterior is given by

$$\begin{split} p(x_1 &= x^* \mid x_t = x) \\ &\propto p(x^*) \cdot p(x_t = x \mid x_1 = x^*) \\ &= p(x^*) \cdot (1 - \alpha_t)^{\text{len}(x^*) - \text{len}(x)} (1 - \gamma_t)^{\# \text{mask}(x)} (\alpha_t + \gamma_t - 1)^{\# \text{unmask}(x)} \cdot \#\{s : x \subseteq x^*|_s\} \\ &\propto p(x^*) \cdot (1 - \alpha_t)^{\text{len}(x^*) - \text{len}(x)} \cdot \#\{s : x \subseteq x^*|_s\}. \end{split}$$

Importantly, as in the vanilla MDM setting, the posterior does not depend on the unmasking schedule (γ_t) (thus β_t), which will enable us to perform unmasking in adaptively chosen positions. Note also that if all sequences in the support of p were of the same length, this posterior would also be independent of (α_t) ; while we do not prove it, in this case this would allow us to choose an arbitrary order of unmaskings and insertions.

Extension of posterior to t=1. Motivated by the form of the posterior above, we define the following:

$$q_t(x^*\mid x) \propto \begin{cases} p(x^*) \cdot \mathbf{1}_{x\subseteq x^*} & \text{if } t=1 \\ p(x^*) \cdot (1-\alpha_t)^{\mathrm{len}(x^*)-\mathrm{len}(x)} \cdot \#\{s: x\subseteq x^*|_s\} & \text{otherwise} \end{cases}$$

Note that for t<1, this is the same as $p(x_1=x\mid x_t=x)$. We will denote the marginals of $q_t(\cdot\mid x)$ by $q_t^i(\cdot\mid x)$ for $v\in\Sigma$. The reason for extending the definition of the posterior to t=1 is that in an adaptive FlexMDM sampler (see Definition E.1), because we are entirely decoupling unmasking from the schedule of insertions, after the final insertion step the time parameter t may be 1 even though there are still tokens left to unmask. We will assume oracle access to $q_1(\cdot\mid x)$ as in practice these are simply the any-order marginals for p, and furthermore in practice these are already well-approximated by the learned posterior marginals $p(x_1^i \cdot \mid x_{1-\delta}=x)$ for arbitrarily small $\delta>0$.

Index-tracking variable. Recall that in the definition of the joint interpolant we defined an index-tracking variable s_t which essentially tracked which indices of x_1 correspond to the tokens in x_t . While our analysis below will not use the language of stochastic interpolants, we will still use the idea of tracking s_t , with slightly modified notation. Specifically, for any $0 \le t < 1$, we will use the notation $\Pr_{(x_1,s)|x_t=x}$ and $\mathbb{E}_{(x_1,s)|x_t=x}$ to denote probability and expectation with respect to the distribution given by sampling x_1 from $q_t(\cdot \mid x)$, and then sampling s uniformly random from subsets for which $x \subseteq (x_1)|_s$. When we only care about the marginal distribution over s, we write $\Pr_{s|x_t=x}$ and $\mathbb{E}_{s|x_t=x}$. Given such a subset s and s and s and s and s are the element in sorted order; as before, we also define the boundary values s and s and s and s are the element in sorted order; as before, we had denoted by $\mathbb{E}[s_t[i] - s_t[i-1] - 1]$ in the main body are thus given by $\mathbb{E}_{s|x_t=x}[s_i - s_{i-1} - 1]$ in the notation of this section.

E.3 FORMAL GUARANTEE FOR ADAPTIVE INFERENCE

Definition E.1. Given query access to the posterior marginals $q_t^i(\cdot \mid x_t = x)$ and to the insertion expectations $\mathbb{E}_{s\mid x_t = x}[s_i - s_{i-1} - 1]$, an adaptive FlexMDM sampler is any algorithm which produces

a sequence of iterates $\hat{x}_{t_1}, \dots, \hat{x}_{t_n}$, where $0 = t_1 < \dots < t_n = 1$, by starting at $\hat{x}_{t_1} = \varepsilon$ and arbitrarily alternating between steps of the following form:

- Any-order unmasking step: Starting from \hat{x}_{t_j} , if $\operatorname{mask}(\hat{x}_{t_j})$ is nonempty, pick an arbitrary index i therein (possibly probabilistically), sample v from $q_{t_i}^i(\cdot \mid \hat{x}_{t_j})$, and set $\hat{x}_{t_j} \leftarrow \hat{x}_{t_j}[\hat{x}_{t_i}^i \leftarrow v]$.
- Insertion step: Starting from \hat{x}_{t_i} , run the CTMC with rate matrix

$$R_t^{\text{ins}}(x,y) = \begin{cases} \mathbb{E}_{s|x_t = x}[s_i - s_{i-1} - 1] \cdot \frac{\dot{\alpha}_t}{1 - \alpha_t} & \text{if } y = x \triangleleft_i \mathbf{m} \\ -\sum_{i=0}^{\text{len}(x)} R_t^{\text{ins}}(x, x \triangleleft_i \mathbf{m}) & \text{if } y = x \\ 0 & \text{otherwise} \end{cases}$$
(9)

for $t_j \le t \le t_{j+1}$ to obtain $\hat{x}_{t_{j+1}}$. If $t_{j+1} = 1$, then apply any-order unmasking until $\operatorname{mask}(\hat{x}_{t_{j+1}})$ is empty, and terminate.

Note that the rate matrix in the second bullet point above is identical to the one in the main body except that we only consider transitions given by insertions.

Formally, we will show the following:

Theorem E.1. Any adaptive FlexMDM sampler for p will generate a sequence of iterates $\hat{x}_{t_1}, \ldots, \hat{x}_{t_n}$ such that \hat{x}_{t_n} is exactly a sample from p.

E.4 PROOF OF THEOREM E.1

To show that adaptive sampling works, we inductively prove an even stronger statement: at any intermediate step of the sampler after it has produced \hat{x}_{t_j} , the final output \hat{x}_{t_n} is a sample from $q_{t_j}(\cdot \mid \hat{x}_{t_j})$.

The following two lemmas provide the inductive steps for unmasking and insertion respectively:

Lemma E.1 (Inductive step for unmasking). Let $0 \le t \le 1$ and let x be a partially unmasked subsequence of length m. Let $\pi = (\pi_i)_{i \in \text{mask}(x)}$ denote any distribution over masked indices of x. Suppose that one runs the following:

- 1. Sample index i from π
- 2. Sample v from the posterior marginal $q_t^i(\cdot \mid x_t = x)$
- 3. Sample from $q_t(\cdot \mid x[x^i \leftarrow v])$.

The output of this procedure is a sample x^* from $q_t(\cdot \mid x)$.

Lemma E.2 (Inductive step for insertion). Let $0 \le t < 1$ and let x be a partially unmasked subsequence of length m. Let $0 \le h \le 1 - t$ be any duration of time. Suppose that one runs the following:

- 1. Starting from x, run the CTMC with rate matrix given by Eq. (9) for time h to obtain x'
- 2. Sample from $q_{t+h}(\cdot \mid x')$.

The output of this procedure is a sample from the posterior $q_t(\cdot \mid x)$.

We defer the proofs of these to Sections E.5 and E.6 below. The idea for the former is identical to the proof of the folklore fact that vanilla MDMs can sample in any order (Kim et al., 2025). The proof for the latter is more involved and involves explicitly verifying that the Kolmogorov *backward* equation is satisfied by the rate matrix we have constructed.

Here we verify that these Lemmas are enough to establish Theorem E.1.

Proof of Theorem E.1. We show more generally that starting from any intermediate time step \hat{x}_{t_j} (not just j=1), any adaptive FlexMDM sampler outputs a sample from $q_{t_j}(\cdot \mid \hat{x}_{t_j})$. We do this by inducting on the total number of insertion steps that remain.

As the base case for the induction, if no more insertion steps remain, then we must have $t_j=1$. In this case, we can further induct on the number of unmasking steps and apply Lemma E.1 with t therein set to 1 to conclude that the final output is a sample from $q_1(\cdot \mid \hat{x}_{t_j})$.

For the inductive step, we have $t_j < 1$ and suppose we have shown that for any FlexMDM sampler that makes at most m insertion steps, starting from any \hat{x}_{t_j} at intermediate time t_j , it samples from $q_{t_j}(\cdot \mid \hat{x}_{t_j})$. Now consider a FlexMDM sampler that makes at most m+1 insertion steps starting from \hat{x}_{t_j} at intermediate time t_j . If in the next step it performs an insertion step, i.e. it runs the CTMC with rate matrix defined above for total time $h=t_{j+1}-t_j$, then by Lemma E.2 and the inductive hypothesis, it samples from $q_{t_j}(\cdot \mid \hat{x}_{t_j})$. Alternatively, suppose the sampler performs some sequence of ℓ unmasking steps before performing an insertion step. Then by further inducting on ℓ , we conclude by Lemma E.1 that the sampler eventually outputs a sample from $q_{t_j}(\cdot \mid \hat{x}_{t_j})$.

Finally, the theorem follows from the special case where $t_j = 0$ and $\hat{x}_{t_j} = \varepsilon$.

E.5 Proof of Lemma E.1

Proof. Fix any index $i \in \text{mask}(x)$. The marginal $q_t^i(\cdot \mid x)$ is given by

$$\Pr_{(x_1,S)|x_t=x}[(x_1)|_{s_i} = v] = \frac{\sum_{x_1,S:(x_1)|_{s_i}=v} p(x) \cdot (1-\alpha_t)^{\operatorname{len}(x_1)-\operatorname{len}(x)} \cdot \#\{S: x \subseteq (x_1)|_S\}}{\sum_{x_1} p(x_1)(1-\alpha_t)^{\operatorname{len}(x_1)-\operatorname{len}(x)} \cdot \#\{S: x \subseteq (x_1)|_S\}}.$$
(10)

The posterior $q_t(\cdot \mid x[x^i \leftarrow v])$ is given by

$$q_t(x^* \mid x[x^i \leftarrow v]) = \frac{p(x^*) \cdot (1 - \alpha_t)^{\operatorname{len}(x^*) - \operatorname{len}(x)} \cdot \#\{S : x[x^i \leftarrow v] \subseteq x^*|_S\}}{\sum_{x_1} p(x_1) \cdot (1 - \alpha_t)^{\operatorname{len}(x_1) - \operatorname{len}(x)} \cdot \#\{S : x[x^i \leftarrow v] \subseteq (x_1)|_S\}}.$$
(11)

Note that the numerator of Eq. (10) and the denominator of Eq. (11) are the same. So conditioned on unmasking index i, the above procedure outputs x^* with probability

$$\begin{split} & \sum_{z} \Pr_{(x_1,S)|x_t=x} [(x_1)|_{s_i} = v] \cdot q_t(x^* \mid x[x^i \leftarrow v]) \\ & = \frac{p(x^*) \cdot (1 - \alpha_t)^{\operatorname{len}(x^*) - \operatorname{len}(x)} \cdot \sum_{z} \#\{S : x[x^i \leftarrow v] \subseteq x^*|_S\}}{\sum_{x_1} p(x_1)(1 - \alpha_t)^{\operatorname{len}(x_1) - \operatorname{len}(x)} \cdot \#\{S : x \subseteq (x_1)|_S\}} \\ & = q_t(x^* \mid x) \,. \end{split}$$

This holds conditioned on unmasking any $i \in \text{mask}(x)$, so regardless of the choice of π over such positions, we will sample from the correct distribution $q_t(\cdot \mid x)$.

E.6 PROOF OF LEMMA E.2

Proof. It suffices to show that the rate matrix satisfies the Kolmogorov backward equation

$$\partial_t q_t(x^* \mid x) = -\sum_{i=0}^{\operatorname{len}(x)} R_t^{\operatorname{ins}}(x, x \triangleleft_i \mathbf{m}) q_t(x^* \mid x \triangleleft_i \mathbf{m}) - R_t^{\operatorname{ins}}(x, x) q_t(x^* \mid x).$$

First note that the rate $R_t^{ins}(x, x \triangleleft_i \mathbf{m})$ can be expressed as

$$\frac{\sum_{x_1} p(x_1) \cdot (1 - \alpha_t)^{\operatorname{len}(x_1) - \operatorname{len}(x)} \cdot \sum_{S: x \subseteq (x_1)|_S} (s_i - s_{i-1} - 1)}{\sum_{x_1} p(x_1) \cdot (1 - \alpha_t)^{\operatorname{len}(x_1) - \operatorname{len}(x)} \cdot \#\{S : x \subseteq (x_1)|_S\}} \cdot \frac{\dot{\alpha}_t}{1 - \alpha_t}.$$

Furthermore, $\sum_{i}(s_i-s_{i-1}-1)=\operatorname{len}(x_1)-\operatorname{len}(x)$, so

$$\sum_{i} R_{t}^{\text{ins}}(x, x \triangleleft_{i} \mathbf{m}) \\
= \frac{\sum_{x_{1}} p(x_{1}) \cdot (1 - \alpha_{t})^{\text{len}(x_{1}) - \text{len}(x)} \cdot \#\{S : x \subseteq (x_{1})|_{S}\} \cdot (\text{len}(x_{1}) - \text{len}(x))}{\sum_{x_{1}} p(x_{1}) \cdot (1 - \alpha_{t})^{\text{len}(x_{1}) - \text{len}(x)} \cdot \#\{S : x \subseteq (x_{1})|_{S}\}} \cdot \frac{\dot{\alpha}_{t}}{1 - \alpha_{t}}.$$
(12)

Let us compute $\partial_t q_t(x^* \mid x)$:

$$-\frac{p(x^{*})\cdot(1-\alpha_{t})^{\operatorname{len}(x^{*})-\operatorname{len}(x)}\cdot\#\{S:x\subseteq x^{*}|_{S}\}\cdot(\operatorname{len}(x^{*})-\operatorname{len}(x))}{\sum_{x_{1}}p(x_{1})\cdot(1-\alpha_{t})^{\operatorname{len}(x_{1})-\operatorname{len}(x)}\cdot\#\{S:x\subseteq(x_{1})|_{S}\}}\cdot\frac{\dot{\alpha}_{t}}{1-\alpha_{t}}$$

$$+\left[\frac{\sum_{x_{1}}p(x_{1})\cdot(1-\alpha_{t})^{\operatorname{len}(x_{1})-\operatorname{len}(x)}\cdot\#\{S:x\subseteq(x_{1})|_{S}\}\cdot(\operatorname{len}(x_{1})-\operatorname{len}(x))}{\sum_{x_{1}}p(x_{1})\cdot(1-\alpha_{t})^{\operatorname{len}(x_{1})-\operatorname{len}(x)}\cdot\#\{S:x\subseteq(x_{1})|_{S}\}}\cdot\frac{\dot{\alpha}_{t}}{1-\alpha_{t}}\right]$$

$$\times\frac{p(x^{*})\cdot(1-\alpha_{t})^{\operatorname{len}(x^{*})-\operatorname{len}(x)}\cdot\#\{S:x\subseteq x^{*}|_{S}\}}{\sum_{x_{1}}p(x_{1})\cdot(1-\alpha_{t})^{\operatorname{len}(x_{1})-\operatorname{len}(x)}\cdot\#\{S:x\subseteq(x_{1})|_{S}\}}$$

$$(13)$$

Note that by Eq. (12), the term in the parentheses in Eq. (13) is exactly

$$\sum_{i=0}^{\mathrm{len}(x)} R_t^{\mathrm{ins}}(x, x \triangleleft_i \mathbf{m}) q_t(x^* \mid x) = -R_t^{\mathrm{ins}}(x, x) q_t(x^* \mid x) ,$$

It remains to verify that the first term in Eq. (13) is equal to $-\sum_i R_t^{\text{ins}}(x, x \triangleleft_i \mathbf{m}) q_t(x^* \mid x \triangleleft_i \mathbf{m})$. To that end, we must show that

$$\sum_{i=0}^{\ln(x)} \frac{\sum_{x_1} p(x_1)(1-\alpha_t)^{\ln(x_1)-\ln(x)} \cdot \sum_{S:x\subseteq(x_1)|_S} (s_i - s_{i-1} - 1)}{\sum_{x_1} p(x_1)(1-\alpha_t)^{\ln(x_1)-\ln(x)} \cdot \#\{S: x_t \triangleleft_i \mathbf{m} \subseteq (x_1)|_S\}} \cdot \#\{S: x \triangleleft_i \mathbf{m} \subseteq x^*|_S\}$$

$$= \#\{S: x \subseteq (x^*)|_S\} \cdot (\ln(x^*) - \ln(x)) \quad (14)$$

The key combinatorial step is as follows. For any x_1 in the support of p, consider a subset S for which $x \subseteq (x_1)|_S$. Note that for every such S, we can uniquely associate exactly $s_i - s_{i-1} - 1$ different subsets S' of size |S| + 1 for which $x \triangleleft_i \mathbf{m} \subseteq (x_1)|_{S'}$. Therefore, $\sum_{S: x \subseteq (x_1)|_S} (s_i - s_{i-1} - 1) = \#\{S: x \triangleleft_i \mathbf{m} \subseteq (x_1)|_S\}$, and the left-hand side of Eq. (14) thus becomes

$$\sum_{i=0}^{\text{len}(x)} \#\{S : x \triangleleft_i \mathbf{m} \subseteq x^*|_S\} = \sum_{i=0}^{\text{len}(x)} \sum_{S : x \subseteq x^*|_S} (s_i - s_{i-1} - 1) = \sum_{S : x \subseteq (x_1)|_S} (\text{len}(x^*) - \text{len}(x_t)),$$

which completes the proof of Eq. (14).

F EXPERIMENTAL DETAILS

F.1 PRETRAINING ON OPENWEBTEXT

Dataset preparation. As mentioned in Section 5.1, to obtain a variable-length dataset, we split OpenWebText articles paragraph-wise using the GPT-2 tokenizer Radford and Wu (2019). This can be implemented by locating the token index corresponding to the delimiter \n \n. Sequences longer than 1024 tokens are then chunked recursively by splitting by the delimiter closest to the middle sequence, yielding a variable-length dataset with maximum sequence length 1024.

FlexAttention. To handle variable-length sequences during training, we pad each batch to the maximum sequence length. In MDM, by design, pad tokens also enter the model input. In contrast, FlexMDM is designed to receive only clean or mask tokens as inputs. Ideally, QKV attention should not attend to pad tokens; however, current FlashAttention (Dao et al., 2022) does not support this for *non-causal* attention (our setup of interest). We therefore adapt FlexAttention (Dong et al., 2024). A side benefit is improved training speed, since FlexMDM performs attention over fewer tokens than MDM's full-sequence attention. Note that in the LLaDA experiment, we did not implement this optimization; pad tokens can therefore attend to other tokens, though we expect the impact to be negligible.

Training configuration. As in Section 5.1, we model FlexMDM with a DiT Peebles and Xie (2023) backbone and embed the insertion schedule α_t . For MDM, we use the same DiT configuration with time step embedding but without the softplus scalar head. Transformer configuration is: hidden size:768, heads:12, conditional dimension:128, dropout:0.05,

layers:12. We train both models on 16 H100 GPUs with a global batch size of 1024 and max training iteration 1M. We use the AdamW (Loshchilov and Hutter, 2017) optimizer with weight decay 0.03, learning rate $3\mathrm{e}{-4}$, 2000 warmup steps, and an EMA factor of 0.9999. Additionally, we use low-discrepancy time-step sampling to reduce variance: one t is drawn uniformly from each interval $[i/T, (i+1)/T]_{i=0}^{T-1}$, as in prior MDM training (Shi et al., 2024).

Metric. For evaluation, we take sequences generated by both models and retain the clean tokens by removing padding (e.g., the leading pad token). We adopt LLaMA-2-7B (Touvron et al., 2023) as the reference model to compute likelihoods. We notice that the pretrained MDM generates short sentences with unreasonably large (worse) perplexities. Therefore, we filter overly short sequences with ≤ 10 tokens when calculating average perplexity.

F.2 PRETRAINING ON THE MAZE PLANNING TASK

Task construction. We generate mazes with a fully random, recursive division procedure (the code is provided in Listing 1), on a 41×41 grid, with some invalid cells. As described in Section 5.1, we consider a subgoal-conditioned planning task: the model is given a sequence of subgoals (g_1, \ldots, g_K) and must produce a valid path that connects them in order. To construct training examples for a given K, we sample 15000 start–goal pairs (g_1, g_K) , compute the shortest path for each pair via breadth-first search, and then add controlled detours to obtain up to 10 distinct valid paths per pair. Subgoals are formed by selecting K-2 intermediate cells uniformly at random along a chosen path (start and goal are already fixed). We use 95% of the pairs for training and hold out 5% for validation to evaluate generalization to unseen pairs and subgoal sets.

Training data construction. For MDM, the training sequence is $((g_1,\ldots,g_K) \ [SEP] \ Path)$, where [SEP] is a special separator and Path denotes the tokenized path. During training, the prompt (g_1,\ldots,g_K) bypasses the interpolant so that, at inference time, the model can condition on (g_1,\ldots,g_K) [SEP] and generate the path. For FlexMDM, we use an interpolant in which the subgoal tokens are exempt from the process in (6); that is, tokens corresponding to each g_i are kept clean at all times. This also enables generation to start from (g_1,\ldots,g_K) . Although this conditional generation template changes the base distributions p_0 for both MDM and FlexMDM, we note that the theoretical guarantee from Section 3 and Section 4 still holds—once the training is perfect (under the access to the ground truth unmasking posterior and insertion expectation), the inference algorithms recover the ground truth distribution p_1 .

Training configuration. We use the same architectural design as in the OpenWebText pretraining, but with a smaller model: hidden size:256, heads:8, conditional dimension:128, dropout:0.1, layers:8. Both models have approximately 8.5M parameters. We train them on 4 A100 GPUs with a global batch size of 256 for up to 100 epochs. We use AdamW (Loshchilov and Hutter, 2017) with weight decay 0.01, learning rate 1×10^{-4} , 20 warmup epochs, and an EMA factor of 0.9999.

Metric. Given the final conditionally generated sequence, we report the success rate under two criteria: (1) all visited cells are valid (no collisions with invalid cells), and (2) the path connects the subgoals consecutively in order. We perform inference both models with the number of sampling steps 256.

Listing 1: Code for the maze Construction

```
q[y, left:left + w] = 1
       g[y, gap] = 0
       _divide(g, top, left, y - top, w)
       \_divide(g, y + 1, left, top + h - y - 1, w)
       x = random.randrange(left + 1, left + w - 1, 2)
       gap = random.randrange(top, top + h, 2)
       q[top:top + h, x] = 1
       g[gap, x] = 0
       _divide(g, top, left, h, x - left)
       \_divide(q, top, x + 1, h, left + w - x - 1)
# WRAPPER with extra doorways -----
# -----
def division_maze(m, n, seed=2025, extra_door_frac=0.5):
   m, n
                    # size in *cells*
                                       (not bitmap coords)
                   # int or None
   seed
   extra_door_frac # 0, perfect maze; >0 flicks more doors (loops)
   random.seed(seed)
   H, W = 2 * m + 1, 2 * n + 1
   g = np.zeros((H, W), dtype=np.uint8)
   g[0, :], g[H - 1, :], g[:, 0], g[:, W - 1] = 1, 1, 1, 1
   \_divide(g, 1, 1, H - 2, W - 2)
    # ----- optional imperfection: punch extra doorways ------
    if extra_door_frac > 0:
       candidates = []
       for r in range (1, H - 1):
           for c in range(1, W - 1):
               if g[r, c] == 1:
                   # Check if wall separates two passages orthogonally
                   if q[r - 1, c] == 0 and q[r + 1, c] == 0:
                       candidates.append((r, c))
                   elif g[r, c - 1] == 0 and g[r, c + 1] == 0:
                       candidates.append((r, c))
       k = int(len(candidates) * extra_door_frac)
       for (r, c) in random.sample(candidates, k=k):
           g[r, c] = 0
    return g
```

F.3 WEIGHT INITIALIZATION TRAINING FROM LLADA

In this section, we describe the procedure for adapting the pretrained LLaDA-8B base model into the FlexMDM.

Training configuration. LLaDA uses a bidirectional Transformer without an additional time embedding, leveraging the fact that MDM does not require an explicit time signal (Zheng et al., 2024). For FlexMDM, to model the insertion expectation, we inject a time-embedding pathway via AdaLN (Peebles and Xie, 2023). For parameter efficiency, we tie (share) the four AdaLN parameter sets across the intermediate Transformer layers. We also attach a softplus scalar head to parameterize the insertion expectation.

Next, we attach LoRA adapters (Hu et al., 2022) to every attention projection (q_proj, k_proj, v_proj) and to the unmasking-posterior head. We include LoRA on the unmasking posterior head because the unmasking posteriors differ between MDM and FlexMDM: in FlexMDM, unmasking must account for token shifts induced by insertions. This fine-tuning of the last head is crucial for enabling variable-length generation.

The LoRA configuration that we use is r=128, $\alpha=128$, and dropout 0.1. Training runs for 200,000 gradient steps with a batch size of 64 on 16 H100s, which took approximately 3 days. We optimize with AdamW (Loshchilov and Hutter, 2017) at learning rate 1×10^{-4} and weight decay 0.1, using a cosine warm-restarts scheduler.

Evaluation on GSM8K. We instruction-fine-tune (IFT) the FlexMDM base model on the GSM8K training split. To preserve the instruction-answer format, we modify the interpolant in Eq. 6 so that tokens corresponding to the instruction are excluded from the interpolant—these tokens remain fixed for all time steps. We apply the same strategy to obtain the baseline (that is, IFT from LLaDA-base), modifying the MDM interpolant so that instruction tokens remain fixed. This choice is equivalent to the IFT recipe used in Nie et al. (2025); Ye et al. (2025). Both models are IFT-ed for 1000 epochs. (Other IFT hyperparameters match those used in our base setup unless otherwise noted.)

For FlexMDM inference, we start from the instruction prompt at t=0 and run adaptive inference to t=1. Concretely, we use Top-K probability with a sliding window (Appendix E) with $\gamma_1=5.0$ and $\gamma_2=64$. For LLaDA, we report the best result under the semi-autoregressive, confidence-based sampling of (Nie et al., 2025). For both models, we set the token sampling temperature to 0.0, which we confirm to be important for strong Pass@1. Overall, adaptive inference substantially improves performance over vanilla inference.

Evaluation on HumanEval-infill. Code infilling conditions on a prefix and suffix, and asks the model to complete the middle part of the code. For FlexMDM, we format training examples as (Prefix; [SEP]; [Middle]; [SEP]; Suffix), where [SEP] is a separator token and Instruction describes the infilling task for a model. We modify Eq. (6) so that tokens for Prefix, Suffix, and [SEP] are fixed in the interpolant (i.e., excluded from the interpolant). Thus, at t = 0 the state is (Prefix; [SEP]; [SEP]; Suffix).

For MDM, we use the format (Instruction; [PRE]; Prefix; [SUF]; Suffix; [SEP]; Middle), with Instruction prompting infill after prefix and suffix, along with [PRE] and [SUF] separate the prefix and suffix, respectively. Here too, the tokens without Middle are held fixed by the modified interpolant. This difference in formatting reflects the fixed-length nature of MDMf MDM (no token insertion). This formatting has been used in the code infilling tasks for autoregressive models in Bavarian et al. (2022). Naively masking the Middle span yields a base state at t=0 of (Prefix; Masked; Suffix), where Masked is a fully masked sequence of length |Middle|. This leaks length information—materially simplifying the task— and renders comparisons to FlexMDM unfair, since FlexMDM does not observe the target span length. For fair evaluation, we therefore avoid length-revealing masks and require methods to infer the span length during inference.

We IFT both models on the educational-instruct split of <code>opc-sft-stage2</code>; the architecture and optimization configurations match those used for GSM8K IFT. At evaluation, we initialize from the base distributions: for FlexMDM, (<code>Instruction;Prefix;[SEP];[SEP];Suffix</code>); for MDM, (<code>Instruction;Prefix;Suffix;[SEP]</code>). We use the same Top-K adaptive inference for both and temperature 0.0. Final outputs are scored with the HumanEval-infill verifier toolkit to compute success rates.